

1 Indian Plate paleogeography, subduction, and horizontal  
2 underthrusting below Tibet: paradoxes, controvercies,  
3 and opportunities

4

5

6

DOUWE J.J. VAN HINSBERGEN

7

8

9

Department of Earth Sciences, Utrecht University, Princetonlaan 8A, 3584 CB

10

Utrecht, the Netherlands. [d.j.j.vanhinsbergen@uu.nl](mailto:d.j.j.vanhinsbergen@uu.nl)

11

12

*This is the third, accepted version of the manuscript, published in NATIONAL*

13

*SCIENCE REVIEW*, <https://doi.org/10.1093/nsr/nwac074>

14

15

16        Keywords

17    Collision, orogenesis, subduction, reconstruction, Himalaya, Tibet

18

## 19    Abstract

20    The India-Asia collision zone is the archetype to calibrate geological responses of  
21    continent-continent collision, but hosts a paradox: there is no orogen-wide geological  
22    record of oceanic subduction after initial collision around 60-55 Ma, yet thousands of  
23    kilometers of post-collisional subduction occurred before arrival of unsubductable  
24    continental lithosphere that currently horizontally underlies Tibet. Kinematically restoring  
25    incipient horizontal underthrusting accurately predicts geologically estimated diachronous  
26    slab break-off, unlocking the Miocene of Himalaya-Tibet as natural laboratory for  
27    unsubductable lithosphere convergence. Additionally, three end-member paleogeographic  
28    scenarios exist with different predictions for the nature of post-collisional subducting  
29    lithosphere but each is defended and challenged based on similar data types. This paper  
30    attempts at breaking through this impasse by identifying how the three paleogeographic  
31    scenario each challenge paradigms in geodynamics, orogenesis, magmatism, or  
32    paleogeographic reconstruction and identify opportunities for methodological advances in  
33    paleomagnetism, sediment provenance analysis, and seismology to conclusively constrain  
34    Greater Indian paleogeography.

35

## 36    Introduction

37        With major continents being too buoyant to subduct – the reason why they can  
38    become billions of years old – colliding continents are associated with subduction arrest,  
39    plate reorganization, and orogenesis (1), seaway closure, mountain building, and  
40    atmospheric barrier formation (2). The orogen at the India-Asia continental collision zone  
41    is the archetype to calibrate the relationships between collision, orogenic architecture,  
42    history, and dynamics, resulting magmatism and mineralization, as well as climatic and

43 biological responses (2-6). But long-standing paradoxes and controversies in tectonic  
44 history have led to an impasse, making using the full potential of the archetype difficult.

45 Geophysical imaging has revealed that Indian continental lithosphere has  
46 horizontally underthrust the Tibetan upper plate (7-12). This is consistent with the  
47 paradigm of unsubductability of thick continental lithosphere (1) and offers opportunities  
48 to study the dynamics of and response to convergence between buoyant lithospheres (13).  
49 But Indian lithosphere only reaches ~400-800 km north of the Himalayan front (7-12)  
50 and according to kinematic reconstructions of Indian plate consumption (9, 11, 14), and  
51 geological estimates of the last slab break-off in the Himalaya (15), accounts for only the  
52 last 25-13 Ma (diachronous along-strike) of India-Asia convergence (9, 14).  
53 Paradoxically, the youngest unequivocal geological records of plate-boundary-wide  
54 oceanic subduction between India and Asia are older than 60 Ma (16-18), after which  
55 more than 4000 km of India-Asia plate convergence occurred (19, 20). So between the  
56 geologically recorded collision and the onset of horizontal underthrusting of Indian  
57 lithosphere, thousands of kilometers of post-collisional subduction occurred.

58 This paradox is not readily explained by dynamic models of continental collision.  
59 These rather portray a process of ~10 Ma, during which a few hundred kilometers of one  
60 continental margin is dragged down below another, causing deformation of both margins,  
61 after which convergence stops, the slab detaches, and the deformed belt rebounds and  
62 uplifts (21). Long-standing controversy in the geological debate on the India-Asia  
63 collision history comes from different solutions to explain this paradox. End-member  
64 solutions fall into three classes that fundamentally differ in post-collisional  
65 paleogeography of the Indian plate. The first end-member predicts that all post-collisional  
66 subduction consumed continental lithosphere (18, 22, 23), and the second and third infer  
67 that after initial collision, oceanic lithosphere remained to the north (6, 24-27), or to the  
68 south (9, 28) of the initial collision zone, which subsequently subducted 'post-collision'.  
69 The former option challenges the paradigm of wholesale continental unsubductability.  
70 While it has become clear that thinned continental lithosphere may become dense enough  
71 to subduct without leading to subduction arrest and slab break-off, e.g. due to  
72 eclogitization during burial, but in numerical experiments (29) as well as in orogens

73 elsewhere (30), the sedimentary upper crust is decoupled from subducted continental  
74 lithosphere and remains behind in orogenic belts. If all of Greater India was continental,  
75 far more continental crust is subducted than suggested by the upper crustal remains found  
76 in the Himalaya, of if true, this is key to advance understanding of geodynamics (23). The  
77 latter options challenge paradigms of orogenic architecture and evolution ensuing from  
78 oceanic subduction (22, 31) and if true, holds key lessons for reconstructing  
79 paleogeography from orogenic archives (30). In all cases, the records of magmatism,  
80 deformation, and topographic rise in Tibet and the Himalaya between the onset of  
81 collision and the onset of horizontal underthrusting occurred in context of, and contain  
82 key information on a-typical subduction, either in terms of the nature of the downgoing  
83 plate, or in terms of the orogenic and magmatic response.

84 In the last decade, the controversy on India's paleogeography has reached an  
85 impasse: each of the end-member scenarios is argued for and against based on the same  
86 types of data, notably sediment provenance constraining upper plate sediments arriving  
87 on lower plate continental margins (6, 9, 18, 32, 33), paleomagnetic data constraining  
88 paleolatitudes of continental margins and arcs (26, 28, 34-37), and seismic tomographic  
89 images revealing locations of past subduction zones (11, 14, 38, 39). Even though the  
90 volume of these databases has rapidly increased in recent years, they have mostly focused  
91 on testing the kinematic and paleogeographic predictions of each endmember model  
92 without leading to a consensus. This paper rather aims to explore the unique opportunities  
93 that each of these endmembers hold for the archetype to challenge and develop  
94 paradigms of geodynamics, orogenesis, and environmental response.

95 This paper aims to (i) attempt at formulating the paradox and explaining the  
96 controversy and the key predictions of each proposed class of explanations; (ii) review  
97 geological constraints on Indian plate subduction provided by the Himalayan mountains  
98 that consist of offscraped upper crustal rocks derived from Indian plate lithosphere and  
99 accreted to the upper plate, and on coeval upper plate geological evolution of the Tibetan  
100 Plateau; (iii) use these constraints to identify which tectonic and magmatic  
101 reorganizations coincide with horizontal Indian underthrusting, and aim to identify the  
102 natural laboratory to analyze the dynamics of non-subductable lithosphere convergence;

103 (iv) discuss ways forward to reconcile existing datasets and find novel ones to break  
104 through the impasse in Greater India paleogeography reconstruction and show the  
105 opportunities that each of the three end-member scenarios would provide in using the  
106 India-Asia archetype to constrain the geological and dynamic consequences of its a-  
107 typical post-collisional subduction.

108

## 109 Review

### 110 The paradox: underthrust versus subducted Indian plate lithosphere

111 A key question in the analysis of the India-Asia collision history and dynamics is  
112 where and how post-collisional convergence has been accommodated. Kinematic  
113 reconstructions have shown that approximately 1000-1200 km of Cenozoic convergence  
114 was accommodated by shortening and extrusion in the overriding plate of Tibet (9, 40,  
115 41). Reconstructing this convergence in the mantle reference frame aligns the southern  
116 Eurasian margin with underlying slabs imaged by seismic tomography, and in the  
117 paleomagnetic reference frame satisfies first-order vertical axis rotations and south  
118 Tibetan paleolatitudes for the Cretaceous and Paleogene (9). This reconstructed  
119 shortening of Tibet is by far the largest amount of intra-plate shortening recorded in post-  
120 Paleozoic orogens (30). Shortening records of the Indian-plate-derived thin-skinned  
121 Himalaya fold-thrust belt give somewhat smaller numbers, between 600-900 km (42). It  
122 is puzzling that post-collisional convergence far exceeds these numbers: the earliest  
123 estimates for post-collisional convergence assumed a 45 Ma collision (40), which would  
124 generate a shortening deficit of ~1000 km, but stratigraphic ages of the oldest foreland  
125 basin clastics in the northernmost continental rocks of the Himalaya, as well as ages of  
126 (U)HP metamorphism in continent-derived rocks in the northern Himalaya has pushed  
127 the estimated initial collision age backward, to ~60-55 Ma (16, 17, 43). India-Asia plate  
128 circuits constrained by magnetic anomalies predict 3500 and 4500 km of post-60 Ma  
129 convergence at the longitude of the western and eastern Himalayan syntaxis, respectively  
130 and (19, 20) (Fig. 1). Much of the post-collisional subduction has thus not left an  
131 accreted rock record, either because of whole-sale subduction, or of (subduction-) erosion  
132 of previously accreted records.

133 Seismological research in the last two decades has painted a detailed image of the  
134 mantle below India and Tibet that helps identifying where lost lithosphere may now  
135 reside. First, lithosphere below Tibet is up to 260 km thick, which was at first surprising  
136 (44): major lithospheric thickening associated with intraplate shortening is predicted to  
137 lead to convective instability of lithosphere, that will then delaminate (45). However,  
138 since then the thick lithosphere below Tibet has become interpreted as horizontally  
139 underthrust Indian crust and continental mantle lithosphere (7-12). Tibetan lithosphere  
140 has indeed delaminated: Indian continental crust appears to directly underlie Tibetan  
141 crust, not intervened by a thick lithospheric mantle (12). In addition, seismic tomographic  
142 evidence for bodies of high-velocity material that may represent delaminated Tibetan  
143 lithosphere have been identified in the upper mantle below the horizontally underthrust  
144 Indian lithosphere, suggesting delamination prior to underthrusting (46). Moreover,  
145 recent seismological analysis has shown that delamination is not restricted to Tibet, but  
146 also affected the Yunnan region to the southeast of the eastern Himalayan syntaxis, where  
147 a conspicuous, circular shaped hole in the continental lithosphere is underlain by a body of  
148 high-velocity material at the base of the upper mantle (47).

149 The first detailed seismological section that detected horizontally underthrust  
150 lithosphere revealed that the Indian continent protrudes ~400 km north of the southern  
151 Himalayan front (12). Since then, multiple seismic tomography models have reproduced  
152 this finding, but showed that the shape of the northern Indian margin is irregular,  
153 protruding ~800 km northward at the longitude of the eastern Himalayan syntaxis,  
154 abruptly stepping southward to the north of Bhutan, and then increasing to ~700 km  
155 again towards the longitude of the western syntaxis (Fig. 2) (7-11). An onset of horizontal  
156 underthrusting can be calculated when assuming that the body of lithosphere below Tibet  
157 is a rigid part of the Indian plate, reconstructing India-Asia convergence, and corrected  
158 for Tibetan shortening. This predicts that the onset of horizontal underthrusting started  
159 around the Himalayan syntaxes around 28 Ma, and becomes gradually younger to ~15  
160 Ma at the longitude of Bhutan (9, 14) (Fig. 3). Geological reconstructions of uplift,  
161 heating, and resulting leucogranite intrusion in the Himalayan mountain range interpreted  
162 to reflect lateral propagation of slab detachment a few Ma after the underthrusting of the  
163 modern Indian crust below Tibet, predicted 25 Ma for the eastern- and westernmost

164 Himalaya, gradually younging towards 13 Ma in Bhutan (15). This match suggests that  
165 the thick body of lithosphere below Tibet is indeed horizontally underthrust Indian  
166 lithosphere.

167 All Indian plate lithosphere that was consumed before Miocene horizontal  
168 underthrusting must thus have subducted into the mantle. There is broad consensus that  
169 the majority of this subducted lithosphere resides in the lower mantle below India, with a  
170 smaller and younger slab that was the last to detach, overturned in the mantle to the north  
171 of the main India slab (Fig. 2) (9, 11, 38, 39, 48). An additional anomaly in the lower  
172 mantle below the equatorial Indian ocean has also long been interpreted as Neotethyan  
173 (28, 38, 39), but may instead be a relict of Mesozoic subduction between Tibetan blocks  
174 (14) (Fig. 2).

175 In summary, the paradox of the India-Asia collision is the following: there is no  
176 geological record of oceanic subduction that spanned the width of the orogen after initial  
177 collision around 60 Ma, and the system is therefore widely believed to have been fully  
178 continental since this time (11, 22, 23); yet thousands of kilometers of Indian plate  
179 lithosphere was consumed without leaving an accretionary record, and subducted deeply  
180 into the mantle, which are both typically associated with oceanic subduction and not  
181 previously demonstrated for continents (30). Only the Indian Plate lithosphere that  
182 arrived in the collision zone in the early to middle Miocene did not steeply subduct, but  
183 instead horizontally underthrust below the upper plate.

184

## 185 [The controversy: scenarios for Indian plate paleogeography and subduction](#) 186 [history](#)

187 The above paradox has led to paleogeographic reconstructions for post-collisional  
188 Greater India that fall into three classes (Fig. 4). The first and most commonly portrayed  
189 scenario (Model C, for Continental) assumes that all post-collisional convergence  
190 consumed continental lithosphere (18, 22, 23, 40). This scenario provides a  
191 straightforward explanation for the absence of accretion of Ocean Plate Stratigraphy  
192 (OPS (49)) after 60 Ma in the Himalayan orogen, but requires thousands of kilometers of  
193 continental subduction, and this subduction must have been accommodated along a

194 continental subduction thrust in the Himalayas (23). The width of continental Greater  
195 India portrayed on published paleogeographic maps differs as function of collision age,  
196 plate circuit, and assumed Tibetan shortening, but predicts Gondwana reconstructions in  
197 which Greater India was conjugate to the entire western Indian margin (23) up to or  
198 beyond the Argo Abyssal Plain (Fig. 4). This Argo Abyssal Plain is of importance  
199 because it recorded Jurassic continental break-up whereby the conceptual ‘Argoland’  
200 continent whose remains now make up much of Indonesia and west Burma, broke off  
201 Australia around 155 Ma, well before the separation of India from Australia around 130  
202 Ma (50). The Argo Abyssal Plane was thus conjugate to a different continent and plate  
203 than India. Based on marine magnetic anomalies and continental extension  
204 reconstructions of the west Australian margin, Gibbons et al. (50) suggested that  
205 Argoland must have continued as far south of the Wallaby Fracture Zone. Model C thus  
206 requires that this interpretation is incorrect.

207 The second scenario (model A, for Arc) points out that between the Himalaya and  
208 continental southern Eurasia, there are ophiolites and intra-oceanic arc rocks, and invokes  
209 that the 60 Ma collision recorded arrival of the north Indian continental margin in an  
210 intra-oceanic subduction zone, followed by obduction of ophiolites and arc rocks onto the  
211 continental margin (6, 16, 24-27). Following this collision, oceanic lithosphere remained  
212 between the initial collision zone and Eurasia, which was consumed until arrival of the  
213 obducted Indian continental margin at the Tibetan trench. Because there is no  
214 accretionary record of post-60 Ma oceanic subduction, the age of this arrival is based on  
215 interpretations of changes in magmatism in Tibet, or an a (contested) youngest age of  
216 marine sedimentation in the Himalaya, at  $40\pm 5$  Ma (6, 25, 27). To explain how Tibet-  
217 derived sediments arrived at the north-Indian margin around 60 Ma, a recent modification  
218 of this model suggested that the north Himalayan ophiolites originated at the south  
219 Tibetan margin in the early Cretaceous, but migrated southward, together with overlying  
220 Tibet-derived sediments, due to opening of a back-arc basin (6). The intra-oceanic arc  
221 scenario thus predicts that part of the post-collisional subduction history consumed  
222 oceanic lithosphere that must have subducted along a trench between the Himalayan  
223 ophiolites and the south Tibetan margin. Additionally, the assumed  $40\pm 5$  Ma collision  
224 age of the obducted Indian margin and Tibet would still require large amounts (up to



225 1000 km at the longitude of Bhutan) of continental subduction prior to horizontal  
226 underthrusting (Fig. 4). The reconstructed width of continental Greater India depends on  
227 the assumed collision age with Tibet, but would bring the north Greater Indian margin  
228 adjacent to most of the west Australian margin up to the Cape Range Fracture Zone, thus  
229 also challenging Gibbons et al.'s (50) Argoland interpretation (Fig. 4).

230 The third scenario (model M, for Microcontinent) invokes that the 60 Ma  
231 collision in the north Himalaya involves a Tibetan Himalayan microcontinent that rifted  
232 and drifted away from Greater India in Cretaceous times, opening a conceptual Greater  
233 India Basin (GIB) ocean in its wake (28). Assuming that the horizontally underthrust  
234 portion of India below Tibet represents the southern paleo-passive margin of this basin  
235 leads to a reconstruction whereby Greater India in Gondwana times did not extend  
236 beyond the Wallaby Fracture Zone of the southwest Australian margin (9), far south of  
237 the Argo Abyssal Plain, but consistent with west Australian margin reconstructions that  
238 interpreted that Jurassic break-up of Argoland to continue to the Wallaby Fracture Zone  
239 (50). This model thus invokes that continental subduction was restricted to only the lower  
240 crustal and mantle underpinnings of the Tibetan Himalayan microcontinent. However,  
241 this model also requires that an oceanic basin was consumed along a subduction thrust  
242 within the Himalayan mountain range without leaving a modern geological record  
243 anywhere in the Himalaya. Finally, this scenario does not require, but also does not  
244 exclude the intra-oceanic arc scenario of Model A – this would merely change the width  
245 of the GIB.

246 Each of these scenarios explains some first-order observations from the Greater  
247 Indian paradox, and satisfies some long-held paradigms in subduction behavior or  
248 orogenesis, but challenges others. And each of these models has been defended as well as  
249 contested based on paleomagnetic, structural geological, stratigraphic, and seismic  
250 tomographic data. Below is a brief review of the geological architecture of the Himalaya  
251 and Tibet that is relevant to identify future research targets to advance the discussion, and  
252 to identify the main geological and geodynamic phenomena that occurred in the time  
253 window of horizontal Indian underthrusting.

254

255 **The constraints: architecture and evolution of the Tibetan-Himalayan orogen**

256 Elements of the Himalayan and Tibetan orogen that play a key role in the  
257 interpretations of its tectonic history since 60 Ma are (i) the accretionary fold-thrust belt  
258 of the Himalaya that was offscraped from now-underthrust/subducted Indian plate  
259 lithosphere ; (ii) a belt of overlying ophiolites, and in the west of the collision zone,  
260 Cretaceous-Eocene intra-oceanic arc rocks that represent the upper plate of an overriding  
261 oceanic lithosphere above a subduction zone; and (iii) continental crust of the Tibetan  
262 plateau that consists of pre-Cenozoic accreted terranes and intervening sutures, intruded  
263 by a Mesozoic-Cenozoic magmatic arc that also shows it was in an upper plate position  
264 above a subduction zone (Fig. 5). These constraints, and how they play a role in the three  
265 scenarios for Indian paleogeography summarized above, are as summarized below.

266

267 **Himalaya**

268 The accretionary fold-thrust belt of the Himalaya consists continent-derived  
269 nappes that underlie of ocean-derived accreted units. These accreted rock units play a key  
270 role in reconstructing subducted plate paleogeography. Conceptually, accreted rock units  
271 fall into two broad types: ocean-derived units consist of Ocean Plate Stratigraphy (OPS),  
272 comprising pillow lavas (MORB, OIB, IAT), pelagic oceanic sediments, and foreland  
273 basin clastics (49). Continent-derived units consist of Continental Plate Stratigraphy  
274 (CPS) that in its simplest form comprises slivers of a basement from an earlier orogenic  
275 cycle, an unconformable cover of syn-rift clastic sediments and volcanics, shallow- to  
276 deep-marine platform to pelagic passive margin carbonates and occasional clastic series,  
277 and foreland basin clastics, although a more complex stratigraphic architecture may form  
278 due to climatic or relative sea level variation or a more complex rifting history of the  
279 continental margin (30). Key for analyzing the collision and accretion history are the  
280 foreland basin clastics: these not only date arrival of the accreted units at a trench, but  
281 also allow fingerprinting the nature of the overriding plate through sediment provenance  
282 analysis. The moment of accretion of thrust slices is bracketed between the youngest  
283 flysch deposits giving a maximum age and, if burial was deep enough, the age of  
284 metamorphism (in subduction setting normally of HP-LT type, except during subduction

285 infancy, when HT-HP metamorphic soles may form (51)) of the accreted units, which  
286 gives a minimum age (30). Finally, in fold-thrust belts with continuous foreland-  
287 propagating thrusting in which almost all subducted lithosphere left its upper crust in the  
288 orogen, the youngest age of foreland basin clastics in the higher nappe tends to be similar  
289 to the oldest age of foreland basin clastics in the next-lower nappe (as for instance in the  
290 Apennines and Hellenides of the Mediterranean region (52)). Conversely, extended  
291 periods of non-accretion and wholesale subduction, or subduction erosion removing  
292 previously accreted rocks, are revealed by age gaps between foreland basin clastics in  
293 adjacent nappes (e.g., in the Japan accretionary prism (49)).

294         The Himalayan fold-thrust belt is commonly divided into four main units, three of  
295 which follow the logic outlined above. The highest units, located below the Indus-  
296 Yarlung ophiolites is a *mélange* that consists of deformed and in places metamorphosed  
297 OPS. These include pillow basalts, cherts that are not older than Triassic in age reflecting  
298 the age of opening of the Neotethys ocean (53), and foreland basin clastics in which the  
299 youngest recognized ages are ~80 Ma (54). The first-accreted units are dismembered  
300 metamorphic sole rocks with ~130 Ma  $^{40}\text{Ar}/^{39}\text{Ar}$  cooling ages that provide a minimum  
301 age for subduction initiation (55). HP-LT metamorphic OPS units found in the *mélange*  
302 below the ophiolites interpreted to have formed during oceanic subduction have ages of  
303 100-80 Ma (43).

304         This OPS-derived *mélange* overlies the Tibetan Himalayan nappe. This nappe  
305 consists of upper Proterozoic to Paleozoic basement, upper Paleozoic syn-rift clastics and  
306 volcanics, a carbonate-dominated passive margin sequence that continues into the  
307 Cenozoic (56), and Paleocene to lower Eocene foreland basin clastics whose age  
308 estimates range from ~61-54 Ma (17, 18, 57). Metamorphic ages of (U)HP-metamorphic,  
309 deeply underthrust equivalents of the Tibetan Himalaya reveal ages suggesting that burial  
310 was underway by 57 Ma (43) and continued until at least ~47 Ma (58). These records  
311 provide evidence that continental lithosphere on the Indian plate arrived in a subduction  
312 zone by ~60 Ma or shortly thereafter.

313         The Tibetan Himalayan nappes overlie crystalline rocks of the Greater Himalaya.  
314 These Greater Himalayan rocks are atypical for accretionary fold-thrust belts in their

315 metamorphic grade as well as their stratigraphy. They consist of upper Proterozoic  
316 sedimentary rocks intruded by lower Paleozoic granitoids, which were both  
317 metamorphosed in Cenozoic times under high-grade metamorphic conditions, up to  
318 partial melting, and intruded by leucogranites (6, 59-61). These rocks underwent  
319 prograde metamorphism from ~50 Ma onward showing they have been part of the orogen  
320 since at least early Eocene time (59, 62). The top of the Greater Himalayan sequence this  
321 likely represent the original stratigraphic underpinnings of the Tibetan Himalayan  
322 sequences (15). Ages recording peak metamorphism become younger from top to bottom  
323 across thrusts within the Greater Himalaya, spanning ages from the Eocene to the early  
324 Miocene (63) and (15) suggested that this suggests step-wise accretion of nappes from  
325 the subducting Indian plate throughout much of the Cenozoic. However, there is no  
326 record of a Mesozoic passive margin stratigraphy or Cenozoic foreland basin clastics in  
327 the Greater Himalayan rocks (6, 61). Because accretion is a top-down process and it is  
328 not possible to accrete the deeper part of the stratigraphy without accreting the shallower  
329 part, it is thus untenable that the Greater Himalayan sequence contains separate, far-  
330 travelled CPS-bearing nappes that were derived from lithosphere paleogeographically to  
331 the south of the Tethyan Himalaya (30). Instead, the downstepping and thrusts likely  
332 reflect slow, post-accretion upper plate shortening and burial as part of the thickening  
333 Tibetan Plateau. The Greater Himalayan sequence is separated from the overlying  
334 Tethyan Himalayan sequence by a ductile shear zone that is known as the South Tibetan  
335 Detachment (STD) that has been active in latest Oligocene to middle Miocene time (59)  
336 and was interpreted as a normal fault accommodating exhumation and channel flow (60)  
337 (Fig. 6) or as an out-of-sequence thrust that displaced the Tethyan Himalayan top relative  
338 to its Greater Himalayan underpinnings (15). These may either have been cut out by the  
339 South Tibetan detachment, which would make the Greater Himalaya a separate nappe  
340 derived from crust that was paleogeographically to the south of the Tibetan Himalaya and  
341 that underthrust below the Tethyan Himalaya in the early Eocene, or it formed the  
342 original stratigraphic underpinnings of the Tethyan Himalaya making them part of the  
343 same nappe.

344           The base of the Greater Himalaya is the Main Central Thrust (MCT) a ductile  
345 shear zone that is the youngest thrust of the Greater Himalayan sequence. It has a

346 downward decreasing metamorphic grade, signalling syn-exhumation activity, that  
347 reveals ages of latest Oligocene to middle Miocene (~26-13 Ma) activity coeval with the  
348 South Tibetan Detachment (59, 60). The coeval activity of the MCT and STD is  
349 commonly (but not exclusively, (15)) interpreted to reflect extrusion of a mid-crustal part  
350 of the orogen (64) that slowly heated up following burial since the Eocene (59). During  
351 Miocene exhumation, the Greater Himalayan crystalline rocks were emplaced onto the  
352 Lesser Himalayan sequence that contain Lower Miocene foreland basin clastics (see  
353 below) and were accreted to the orogen since the Middle Miocene.

354         The Lesser Himalaya consists of a Proterozoic, Paleozoic and older, low-grade  
355 metasedimentary, and discontinuous Cretaceous to Paleocene clastic sedimentary rocks,  
356 in places overlain by Eocene and Miocene foreland basin clastics (57). Upper Cretaceous  
357 to Eocene clastic sedimentary rocks become more prominent towards the west, in  
358 Pakistan, where Eocene and younger foreland basin clastics are also found on the  
359 undeformed Indian continent (65, 66). The provenance of Upper Cretaceous and Eocene  
360 foreland basin clastics in the Lesser Himalayas and on the NW Indian continent reveal  
361 erosion of Indian margin rocks and ophiolites that signal Eocene or older obduction, and  
362 is commonly interpreted to reflect collision recorded in the Tethyan Himalaya to the  
363 north (33, 57, 65, 66). However, the western margin of India was also the locus of  
364 orogenesis due to ophiolite emplacement, in a Late Cretaceous and an Eocene phase, but  
365 this obduction was governed by convergence between the Indian and Arabian plates and  
366 the collision of the Kabul microcontinent with west India (67). So far, the sediment  
367 provenance studies have not identified whether the west and north Indian margin have  
368 distinctly different signatures presenting an unresolved challenge in interpreting sediment  
369 provenance (9). Duplexing of the Lesser Himalayan rocks occurred in the last ~15-13 Ma  
370 and accounted for hundreds of kilometers of shortening that is similar to  
371 contemporaneous Indian plate consumption (42, 68).

372         The structure of the Himalaya summarized above show an overall foreland  
373 propagating fold-thrust belt, but with a clear omission of accretion between the Eocene  
374 (Tibetan and Greater Himalaya) and Miocene (Lesser Himalaya). There are two end-  
375 member interpretations of this hiatus in accretionary record. Before their Miocene

376 emplacement onto the Lesser Himalaya, the rocks exposed in the Greater Himalaya must  
377 have been overlying rocks that have now been transported farther below the orogen and  
378 the nature of these rocks is unknown. On the one hand, these rocks may have been the  
379 original underlying Indian basement (22, 68) (Fig. 7). In that case, there has been no net  
380 convergence between the Greater and Lesser Himalaya between Eocene burial of the  
381 former and Miocene burial of the latter. The Eocene-Miocene India-Asia plate boundary  
382 must then have been located north of the Himalaya. Of the three models for Indian  
383 paleogeography (Fig. 4), only Model A (intra-oceanic arc) could allow for this scenario:  
384 in that case, early Eocene burial of the Greater Himalaya follows upon obduction, and  
385 activation of the MCT would reflect final collision of the obducted margin with Tibet –  
386 but this would require a diachronous Miocene collision age, instead of the proposed  $40\pm 5$   
387 Ma collision ages. All other scenarios require that a subduction plate boundary (intra-  
388 continental, or ocean-below continent) existed within the Himalaya. In that case, the  
389 Greater Himalayan sequence must have decoupled from its Indian basement sometime  
390 after its early Eocene arrival in the orogen, and subsequently formed part of a slowly  
391 thickening and heating orogen. This may be consistent with the evidence for  
392 downstepping thrusting and progressively younger metamorphic ages from top to bottom,  
393 throughout the Paleogene (15, 63). The activation of the Miocene MCT was then the  
394 youngest of these downstepping thrusts and decoupled the modern Greater Himalayan in  
395 the hanging wall from its pre-Miocene underpinnings that traveled deeper below the  
396 orogen, followed by accretion of the Lesser Himalayan foreland basin and deeper  
397 stratigraphic units. Such a scenario is typically implied in numerical simulations of  
398 Himalayan extrusion and channel flow (69) and interprets the MCT, and the older intra-  
399 Greater Himalayan thrusts, as out-of-sequence thrusts in a shortening and thickening  
400 upper plate (Fig. 7). Importantly any Eo-Oligocene accretionary record and associated  
401 thrusts that formed below the Greater Himalayan sequence were then removed from the  
402 orogen, i.e. essentially through subduction erosion (70), upon activation of the MCT (Fig.  
403 7). In Model C and A, this removed part of the orogen consisted of accreted CPS, in  
404 Model M (microcontinent), it may also have included OPS.

405

406 Indus-Yarlung ophiolites and Kohistan-Ladakh arc

407 Overlying the accretionary orogen of the Himalaya are a series of ophiolites  
408 concentrated in a narrow belt along the northern Himalaya (6) (Figs. 5 and 6). These  
409 'Indus-Yarlung' ophiolites are predominantly Early Cretaceous in age (~130-120 Ma),  
410 during which time they formed by extension in the forearc above a (presumably  
411 incipient) subduction zone (6, 55). In some places also older, Jurassic oceanic crust is  
412 found in ophiolites, which may reflect the ocean floor trapped above the subduction zone  
413 in which the Cretaceous ophiolites formed (6). In addition, in the western Himalaya, a  
414 long-lived intra-oceanic arc sequence (150-50 Ma) that is located between the ophiolites  
415 and the continental units of southern Eurasia is known as the Kohistan-Ladakh arc (71).  
416 These sequences showed that the accretion of the Himalayan rocks occurred below a  
417 forearc that consisted of oceanic lithosphere, which plays a central role in the controversy  
418 about Greater Indian paleogeography.

419 The Kohistan-Ladakh arc is overlain by a Cretaceous to Eocene sedimentary  
420 sequence and is separated from Tibetan continental rocks by the Shyok Suture (Fig. 5).  
421 Convergence across this suture zone has been proposed to be either significant and  
422 continuing to Eocene time (26, 27) or minor and pre-dating the late Cretaceous (32), but  
423 in any case testifies to the existence of a paleo-subduction zone between the Kohistan-  
424 Ladakh arc and Eurasia. The Indus-Yarlung ophiolites are overlain by sediments of the  
425 Xigaze forearc basin that form a major syncline with 4-5 km of sediments along 550 km  
426 of the subduction zone (72, 73). The oldest sediments are ~130 Ma old and  
427 unconformably overlie exhumed oceanic core complexes of the ophiolites and elsewhere  
428 interfinger with the ophiolites' pelagic sedimentary cover (74), and the youngest part of  
429 the continuous section is ~50 Ma (72, 73). Low-temperature thermochronology revealed  
430 that the succession may have been almost twice as thick and suggested that sedimentation  
431 and burial may have continued until ~35 Ma (72). The Xigaze forearc has been shortened  
432 along the north-dipping Gangdese Thrust, which brought Tibetan rocks over the forearc  
433 between ~27 and 23 Ma (75), and the Great Counter thrust that backthrusted the Xigaze  
434 forearc over the south Tibetan margin between ~25 and 17 Ma (6) (Fig. 6). Sediment  
435 provenance studies of the Xigaze forearc sequence typically depict southern Tibet and its  
436 overlying magmatic arc as source (72-74), although others prefer an intra-oceanic arc

437 derivation (25, 26) and there is no known accretionary record of OPS or melange along  
438 the strike of the Xigaze forearc basin that may reflect the location of a post-60 Ma  
439 paleosubduction zone.

440         The Indus-Yarlung ophiolites have been interpreted as the forearc of the Eurasian  
441 plate, whereby they formed by (hyper)-extension of the Tibetan continental lithosphere,  
442 occasionally trapping ocean floor that existed before subduction initiation next to the  
443 south Tibetan passive margin (76, 77). In this case, the Kohistan-Ladakh arc forms an  
444 along-strike, offshore continuation of a contemporaneous arc in Tibet (the Gangdese arc,  
445 Fig. 6) and the Shyok suture accommodated only minor convergence that eastwards was  
446 accommodated within the Tibetan Plateau (9, 32). This scenario is required by Model C  
447 (fully-continental Greater India), and preferred by model M (microcontinent). On the  
448 other hand, Model A predicts that the Kohistan-Ladakh arc and Indus-Yarlung ophiolites  
449 formed at (or migrated to (6)) equatorial latitudes, far south of the south Tibetan margin,  
450 at a separate subduction zone (25-27) from the south Tibetan active margin. This model  
451 predicts major convergence across the Shyok Suture, but requires that a long-lived  
452 subduction zone is hidden between the Xigaze Basin and the adjacent south Tibetan  
453 margin.

454

#### 455 Tibetan Plateau

456 The Tibetan Plateau consists of a series of Gondwana-derived continental fragments and  
457 intervening suture zones that amalgamated in Mesozoic time (6, 78). The southernmost of  
458 these fragments is the Lhasa Block that accreted to the Tibetan Plateau in early  
459 Cretaceous time (6, 78), around the same time as the formation of the south Tibetan  
460 ophiolites above a nascent subduction zone to the south of Lhasa (55). Shortening of the  
461 Tibetan upper plate above this subduction zone already started in late Cretaceous time  
462 (79-81), and amounted perhaps already 400 km before initial collision (41) in addition to  
463 the 1000-1200 km of post-60 Ma shortening (9, 41). Detailed stratigraphic records reveal  
464 that shortening in the plateau may have been pulsed, but there is no evidence of a  
465 shortening pulse associated with initial collision around 60 Ma; the recorded pulses may  
466 rather reflect changes in Indian subduction rate (20, 80). In Eocene-Oligocene time,



467 shortening was concentrated in the central Tibetan Plateau. Sometime in late Eocene or  
468 Oligocene time ( $\sim 30 \pm 7$  Ma), Tibetan shortening started to affect the southern margin of  
469 the rigid Tarim block to the north of the modern Plateau. To the west of this block,  
470 Eurasian lithosphere started to subduct southward, accommodated along the Kashgar-  
471 Yecheng transform fault, whereas to the southeast of Tarim, Tibetan crust started to move  
472 NE-ward along the Altyn Tagh fault (82). In late Oligocene time,  $\sim 25$  Ma, shortening  
473 propagated beyond the Tarim block into the Tien Shan, intensifying at  $\sim 13$ -10 Ma (83).  
474 Throughout this history, also NE Tibet underwent outward growth by foreland-  
475 propagating thrusting (6, 84).

476 Paradoxically, even though the Tibetan Plateau and Tien Shan underwent ongoing  
477 shortening in Oligocene to Early Miocene time, south-central Tibet experienced dynamic  
478 subsidence, or even extension. On the southern margin of the Lhasa block, close to the  
479 suture zone, formed the 1300 km long Kailas Basin, which forms a southward thickening  
480 wedge of  $>3$  km of sediments whose architecture and sedimentology suggests it formed  
481 in the hangingwall of a north-dipping normal fault, even though the fault itself is not  
482 exposed, perhaps cut out by the Great Counter Thrust (85, 86) (Fig. 6). The stratigraphy  
483 in any section of the basin accumulated within only 2-3 Ma, but the timing of basin  
484 formation propagates diachronously along-strike, between 26 and 24 Ma in the west, and  
485 becoming as young as 18 Ma in the east (86).

486 Upper plate deformation also involved lateral extrusion (40). In the east of the plateau,  
487 crust was extruded eastwards already in the Eocene, first accommodated by rotations and  
488 thickening in northwest Indochina and later, sometime between  $\sim 30$  and 15 Ma also by  
489 motion of entire Indochina along the Red River Fault (87) (Fig. 5). In western Tibet, a  
490 similar process may have played a role, although the lack of detailed knowledge of the  
491 geology of Afghanistan limits constraints (24). A recent reconstruction of Central Iran  
492 (88) pointed out major late Cretaceous to Eocene mobility and E-W convergence across  
493 the east Iranian Sistan suture requires that continental fragments of Afghanistan may have  
494 undergone major westward displacement (Fig. 5). Restoring such displacement would  
495 bring the Aghanistan fragments north of the Kohistan-Ladakh arc and is thus relevant in

496 interpreting its paleolatitudinal history in terms of Greater Indian paleogeography, but  
497 awaits future detailed constraints.

498 Around 15-10 Ma, a prominent change in deformation of the Tibetan Plateau occurred,  
499 which most famously marks the onset of regional E-W extension in the plateau interior  
500 (89, 90) (Fig. 6). Towards the west, this extension is bounded by the Karakoram Fault  
501 that accommodated ongoing convergence in the Pamir region (41) (Figs. 5 and 6) and to  
502 the east, it is accommodated by E-W shortening in the Longmenshan range, and by a  
503 deflection of motion towards the Yunnan region in the southeast, accommodated along  
504 major strike-slip faults (2, 90). This motion is prominent today as reflected by GPS  
505 measurements. Eastward surface motion components increase from near-zero at the  
506 Karakoram Fault eastward to a maximum of ~2 cm/yr on the central plateau (91).  
507 Eastward motion components then decrease further to the east due to an increasing  
508 southward velocity component in eastern Tibet, as well as E-W shortening in the  
509 Longmenshan (90, 91). The extension of the plateau interior and the motion of crust  
510 towards the southeast is widely interpreted as driven by excess gravitational potential  
511 energy resulting from plateau uplift (2, 45), facilitated by a partially molten middle crust  
512 (92). The trigger of extension is thought to reflect middle Miocene uplift of Tibet due to  
513 lithospheric delamination (2, 45, 90), or due to Indian continental underthrusting (13).

514 Finally, the Lhasa terrane contains the prominent Gangdese batholith that  
515 represents a long-lived volcanic arc (6) (Fig. 6). Arc magmatism in the Lhasa terrane  
516 related to Neotethys closure has been active since at least early Cretaceous time and  
517 perhaps longer (6). Magmatism of the Gangdese arc since early Cretaceous time  
518 contained flareups and periods of reduced activity, but was mostly active until ~45-40  
519 Ma, after which there was a lull until 25 Ma (3, 6). During this lull, potassic and  
520 ultrapotassic magmatism was active in the Qiangtang terrane, hundreds of kilometers to  
521 the north of the Gangdese batholith, after which magmatism resumed in the Lhasa  
522 terrane, ultrapotassic or shoshonitic/adakitic in composition (3, 6), associated with  
523 economic porphyry copper deposits (4). Since 20 Ma such magmatism also resumed in  
524 the Qiangtang and adjacent Songpan Garzi zones of the Tibetan Plateau (3). Interestingly,  
525 this Miocene magmatism in the Lhasa terrane migrated eastward, 25-20 Ma in western

526 Tibet but 15-10 Ma in the east, towards the longitude of Bhutan (5). The chemistry of  
527 these magmatic rocks is interpreted to be mostly derived from a previously subduction-  
528 enriched asthenospheric source that became stirred by the underthrusting continental  
529 Indian lithosphere (3-5).

530

## 531 Discussion

### 532 Opportunities, 1: Natural laboratory of converging unsubductable lithospheres

533 The kinematic reconstruction constraining of horizontal continental underthrusting of the  
534 Indian continent below Tibet identifies (only) the Miocene and younger history of the  
535 Tibetan-Himalayan geological history as natural laboratory for the convergence of  
536 unsubductable lithospheres. While and extensive analysis of the dynamics of this system  
537 is beyond the scope of this paper, several first-order temporal and spatial relationships  
538 between horizontal underthrusting and geological evolution are clear and may be used as  
539 basis to discern between existing hypotheses, or develop new.

540 Most importantly, the irregular shape of the seismically imaged northern Indian  
541 continental margin shows that initial horizontal underthrusting must have been  
542 diachronous: the coinciding age estimates from the kinematic restoration of this margin  
543 (14) (Fig. 3) and geological estimates of the youngest phase of slab break-off from the  
544 Himalaya (15) of ~25 Ma at the Himalayan syntaxes, decreasing to ~13 Ma in at the  
545 longitude of Bhutan, may provide means to discern between the effects of horizontal  
546 underthrusting and unrelated events. For instance, the re-initiation of magmatism between  
547 25 and 8 Ma in the Lhasa terrane follows the same age progression, lending independent  
548 support to the interpretation that magmatism resulted from incipient Indian continental  
549 lithosphere plowing through and stirring of a previously subduction-enriched  
550 asthenosphere (3-5, 93). On the other hand, Miocene magmatism farther north in the  
551 Tibetan plateau that started around 20 Ma is located far away from the horizontally  
552 underthrusting northern Indian continental margin, and does not show a lateral age  
553 progression, making a direct link unlikely.

554 The formation and deposition of the Kailas basin follows the same diachronous trend, but  
555 precedes the reconstructed slab break-off by a few Ma (86). The recognition of  
556 diachronous initial horizontal underthrusting allows explaining this trend, as well as the  
557 apparent paradox of N-S extension in the Kailas Basin of southern Tibet (85, 86) and the  
558 coeval ongoing upper plate shortening in the Pamir, along the Altyn Tagh fault, and in  
559 NE Tibet (82, 84). The subsidence of the Kailas basin is well explained as the result of  
560 negative dynamic topography, or even upper plate extension, caused by the Himalayan  
561 slab retreating and steepening relative to the upper plate, which was previously  
562 interpreted to reflect slab roll-back (86, 94). Slab roll-back, however, would lead to slabs  
563 horizontally draping the upper-lower mantle transition zone, whereas the Himalaya slab  
564 is overturned northward, which requires slab advance during subduction, prior to  
565 detachment (14) (Fig. 8). But slab advance resisting upper plate retreat would generate  
566 the same relative slab-upper plate motion as envisaged before for Kailas (86, 94). This  
567 resistance only occurs where the slab is still attached, explaining diachroneity in Kailas  
568 Basin formation and its subsequent uplift. But where slab detachment had already  
569 occurred, i.e. at the longitude of the Himalayan syntaxes, the Pamir and eastern Tibet,  
570 horizontal Indian underthrusting may already have caused enhanced friction to drive the  
571 apparently paradoxical simultaneous upper plate shortening and extension (Fig. 8).

572 The reconstructed horizontal Indian underthrusting also sheds light on the long-standing  
573 debate on the trigger of E-W extension in Tibet. There is widespread consensus that this  
574 extension reflects the gravitational collapse of the Tibetan Plateau (2, 13, 45, 90),  
575 alongside orogen-parallel extension in the Himalaya due to oroclinal bending (15). As  
576 final trigger to drive collapse, lithosphere delamination of south-central Tibet (2, 45, 90)  
577 or enhanced plateau uplift due to horizontal Indian underthrusting (13) have been  
578 suggested. Horizontally underthrust Indian continental lithosphere directly underlies  
579 Tibetan crust, and its lithospheric mantle must thus have delaminated prior to the 25 Ma  
580 onset of horizontal underthrusting in western and eastern Tibet. In addition, not only the  
581 source area below the Tibetan Plateau, but also the 'sink' of Middle Miocene and  
582 younger crustal motion in the Yunnan region has undergone lithospheric delamination  
583 (47). This suggests that the 15-10 Ma onset of E-W extension was likely not triggered by  
584 delamination. More likely, collapse was driven by the final onset of horizontal

585 underthrusting below the entire plateau following final slab break-off (13). If horizontal  
586 underthrusting indeed caused uplift, the easternmost part of the Indian continental  
587 promontory north of the eastern syntaxis may have first formed a barrier against plateau  
588 collapse, which was only overcome after the entire Tibetan Plateau became horizontally  
589 underthrust by India since middle Miocene time.

590 Also middle Miocene changes in the Himalaya may be studied in context of the transition  
591 from subduction to horizontal underthrusting. Webb et al. (15) already interpreted syntaxis  
592 formation and Himalayan oroclinal bending as result of the change to horizontal  
593 underthrusting. Also the transition from extrusion of the Greater Himalayan crystalline  
594 rocks along the STD and MCT, to duplexing of the Lesser Himalayan nappes appears to  
595 coincide with the transition to horizontal underthrusting, but future analyses may test  
596 whether there was diachroneity in these processes. The coincidence of intraplate  
597 deformation events, e.g. in the Tien Shan with the onset of horizontal underthrusting in  
598 western Tibet around 25 Ma, and along the entire Tibetan margin around 13 Ma, may  
599 suggest a causal relationship linking convergence between unsubductable lithosphere to  
600 intraplate deformation. On the other hand, the shortening in the Tien Shan may also be a  
601 natural northward progression of intraplate deformation that had long been ongoing in the  
602 Tibetan plateau. Future numerical experiments may test such dynamic hypotheses built  
603 on the Miocene Tibetan-Himalayan natural laboratory for the convergence of  
604 unsubductable lithosphere.

605

## 606 [Opportunities, 2: Improving methodology to unlock the post-collisional](#) 607 [subduction laboratory](#)

608 The ongoing controversy of Greater Indian paleogeography currently hampers using the  
609 interval between initial collision, around 60 Ma, and the 25-13 Ma of horizontal Indian  
610 underthrusting as a conclusive natural laboratory for post-collisional subduction.

611 Regardless of which of scenarios of Model C, A, or M will turn out to be correct, if any,  
612 this natural laboratory holds great promise. Models C and A so far offer no explanation  
613 for why there was a transition from subduction to horizontal underthrusting, or what

614 caused the diachroneity of that transition, but if these scenarios are correct, that  
615 explanation must provide a unique constraint on the subductability of continental  
616 lithosphere. Moreover, Models C and A predict that continental subduction is also  
617 possible without preservation of upper crustal units, or with large-scale subsequent  
618 removal of accreted continental crust through subduction erosion. If these models are  
619 correct, it is thus possible that paleogeographic reconstructions strongly underestimate  
620 the paleogeographic area occupied by continental lithosphere. In fact, if large portions of  
621 continental lithosphere can subduct without leaving a geological record, accreted  
622 geological records such as in the Tibetan Himalaya cannot provide conclusive constraints  
623 on initial collision, but only give a minimum age (30). Finally, model C (since 60 Ma)  
624 and model A (since  $40\pm 5$  Ma) would provide the opportunity to calibrate magmatic  
625 responses to continental subduction.

626 The subduction history of model M is on par with the geodynamic and paleogeographic  
627 paradigm that continental lithosphere generally does not subduct, and that if it does, its  
628 upper crust will accrete in orogenic belts (29, 52). The short-lived, late Paleocene to early  
629 Eocene phase of microcontinental lower crust and mantle lithosphere subduction  
630 combined with upper crustal accretion is an example of the latter. In model M, upper  
631 crustal nappes of all subducted or horizontally underthrust continental lithosphere still  
632 remain in the Himalayan orogen (9). The transition from subduction to horizontal  
633 underthrusting in model M is simply caused by the change from oceanic to continental  
634 subduction. But model M invokes that the anomalous magmatic history of Tibet between  
635 45 and the 25 Ma onset of horizontal underthrusting occurred during oceanic (perhaps  
636 flat slab (9, 86)) subduction and would thus allow calibrating possible magmatic arc  
637 expressions of anomalous oceanic subduction.

638 The three models provide strongly different boundary conditions and have far-reaching  
639 consequences for the analysis of the dynamic drivers of upper and intraplate deformation,  
640 the causes of rapid plate motion changes of India, or the causes and paleogeographic  
641 context of terrestrial biota exchange and radiation. It is therefore important to attempt at  
642 breaking through the impasse in Greater Indian paleogeography reconstruction.

643 The only quantitative constraint on paleogeographic position comes from paleomagnetic  
644 data providing paleolatitudinal control. Paleomagnetic analyses on rocks derived from  
645 Greater India such as the Tibetan Himalayan sequence, of ophiolites and intra-oceanic  
646 arcs and their cover, and of the Lhasa terrane of southern Tibet in principle allows  
647 discerning between Model C, A, and M. But each of these models has been defended and  
648 and challenged based on paleomagnetic data (26, 28, 34-37). So are paleomagnetic data  
649 inconclusive? Rowley (34) recently pointed out that the widely used method to compare  
650 paleomagnetic study means ('paleopoles') with apparent polar wander paths that provide  
651 the global reference against which these data are compared and that are based on  
652 averages of study means, is indeed barely conclusive. The paleopoles underlying APWPs  
653 are scattered by  $\sim 20^\circ$  around the mean, and Rowley (34) argued that individual  
654 paleopoles cannot constrain paleolatitude at a higher resolution. Vaes et al. (95),  
655 however, recently analyzed the source of this scatter, and showed that alongside common  
656 paleomagnetic artifacts such as undersampling of paleosecular variation, and inclination  
657 shallowing in sediments, scatter is predominantly caused by the degree to which  
658 paleosecular variation is averaged: scatter is a function of the number of paleomagnetic  
659 datapoints used to determine a paleopole. And because this number is arbitrary, the  
660 statistical properties of APWPs calculated from paleopoles are arbitrary. Vaes et al. (95)  
661 provided a way forward in which paleopoles are compared to a reference curve that is  
662 also calculated from paleomagnetic spot readings rather than paleopoles, and developed a  
663 comparison metric that demonstrates a paleolatitudinal difference or vertical axis rotation  
664 with 95% confidence. This would provide a means to compare datasets of unequal  
665 magnitude and propagate uncertainties, and may provide a more conclusive, quantitative,  
666 and robust paleomagnetic analysis that may discern between the Greater Indian  
667 paleogeography models. Applying this analysis will likely decrease the scatter in  
668 paleomagnetic estimates of paleolatitude, provide more realistic error margins to discern  
669 relative motion between Himalayan units and India, and will demonstrate with a 95%,  
670 rather than a  $\sim 50\%$  certainty whether a difference between a paleopole from the collision  
671 zone and India or Eurasia demonstrates tectonic motion, or not.

672 Models C, A, and M each invoke that a plate boundary must have existed south of the  
673 Tibetan Plateau between the Paleocene to Early Eocene accretion of the Tibetan and

674 Greater Himalayan units in the orogen, and the accretion of the Miocene Lesser  
675 Himalayan units. If this plate boundary was located in the Himalayas during all or some  
676 of the period between 60 and 25/13 Ma, as currently required by all three scenarios, there  
677 may be no record due to out-of-sequence thrusting along the MCT removing the pre-  
678 Miocene underpinnings (Fig. 7). But this refocuses the attention on the process of  
679 extrusion and channel flow, this time not to explain the presence of the Greater  
680 Himalayan rocks in the orogen, but to explain the absence of its pre-Miocene  
681 underpinnings. In addition, Models C and A require that a subduction plate boundary was  
682 present between the Xigaze forearc and underlying ophiolites, and the Lhasa terrane (6).  
683 Detailed mapping, or identifying structures that could explain the lack of a record such as  
684 for the MCT (Fig. 7), may establish whether, when, and where such a subduction zone  
685 may have existed.

686 Also sediment provenance studies have been used to argue for and against Models C, A,  
687 and M. Part of this may underlie the qualitative nature of comparing e.g. detrital  
688 geochronology peaks between the sedimentary record of a sink and a suspected source  
689 area, and recently developed quantitative approaches that identify the likelihood of the  
690 contribution of a given source area to a sediment may advance the discussion (96). In this  
691 analysis, the range of possible source areas for sediments, particularly for Eocene  
692 stratigraphic records in the NW Lesser Himalaya and the Pakistani foreland should  
693 include not only the Himalaya-Kohistan-Ladakh-Tibetan orogen at the India-Asia plate  
694 boundary, but also the Sulaiman-Kabul Block orogen and associated ophiolites that  
695 formed independently at the India-Arabia plate boundary (67) (Fig. 4). In addition,  
696 provenance studies may benefit from broadening the time and space windows of the  
697 investigation. For instance, Triassic sandstones of the northeastern Tibetan Himalaya  
698 were interpreted to have a provenance of western Australia rather than northern Australia  
699 (97), but this conflicts with the interpretation that lower Eocene sediments in the Lesser  
700 Himalaya and on the Indian foreland include sediments derived from the north of the  
701 Shyok Suture (33). Paleogeographic predictions like those for models C, A, and M show  
702 the paleogeographic implication farther back in time of interpretations for the Cenozoic,  
703 and including these in the analysis may resolve apparent conflicting interpretations based  
704 on the same data types (33, 97).



705 Seismic tomographic records of subducted slabs are useful in identifying regions of  
706 paleo-subduction (38, 39), although global correlations suggest that the lower mantle  
707 hosts slabs of the last ~250 Ma (48). Analysis of mantle structure should hence be done  
708 in context of Mesozoic and Cenozoic subduction history and uncertainties therein (14)  
709 (Fig. 2). Nonetheless, a recent seismological study of a slab below Kamchatka was able  
710 to identify thick crust, on the order of 20 km, in a lower mantle slab (98). Once a slab can  
711 be firmly tied to lithosphere that subducted after initial collision, such as the overturned  
712 Himalayan slab that straddles the transition zone (11, 38), such seismological analyses  
713 may provide novel constraints on their composition and crustal nature.

714 In summary, on the one hand, the current controversy on Indian paleogeography  
715 stemming from the inability of geological and geophysical techniques to conclusively  
716 identify between vastly different paleogeographic scenarios, stands in the way of using  
717 the India-Asia collision zone to calibrate the geological and dynamic responses to post-  
718 collisional subduction. On the other hand, this controversy provides the opportunity (and  
719 requires) to question and improve geological methodology to constrain paleogeography,  
720 including orogen structure, sediment provenance analysis, and paleomagnetism. Solving  
721 those issues have impact far beyond the analysis of the India-Asia collision history.

722

## 723 Conclusions

724 Seismological images reveal that 400-800 km of Indian continental lithosphere is  
725 currently horizontally underthrust below Tibet. Using plate reconstructions that  
726 incorporate Tibetan shortening predict that the onset of horizontal underthrusting started  
727 around 25 Ma around the Himalayan syntaxes, gradually younging to 13 Ma at the  
728 longitude of Bhutan. This reconstruction coincides with independent estimates of  
729 diachronous slab break-off in the Himalaya, and identifies the Miocene history of Tibet  
730 as a natural laboratory for convergence of unsubductable lithospheres. This time period  
731 was marked by major changes in accretionary style in the Himalayas, including the  
732 extrusion of the Greater Himalayan crystalline rocks and the transition to Lesser  
733 Himalayan duplexing, but also by the onset of E-W extension and collapse of the Tibetan

734 Plateau, and upper plate shortening reaching as far north as the Tien Shan. Also marked  
735 changes in magmatism in southern Tibet, and associated economic mineralizations  
736 spatially and temporally correlate with the reconstructed inception horizontal  
737 underthrusting. These processes may provide key ingredients of the natural laboratory for  
738 convergence of unsubductable lithosphere. Importantly, lithospheric delamination of  
739 Tibet, often cited as potential trigger for Miocene Tibetan uplift and collapse, must  
740 instead have occurred prior to horizontal Indian underthrusting, hence before the  
741 Miocene.

742 Between initial collision recorded in the Himalaya at 60 Ma and the onset of horizontal  
743 Indian underthrusting, thousands of kilometers of subduction consumed Indian plate  
744 lithosphere. Three end-member scenarios invoke that all or part of this lithosphere was  
745 continental, challenging geodynamic and paleogeographic reconstruction paradigms, or  
746 that most of this lithosphere was oceanic, challenging magmatic and orogenic  
747 architecture paradigms. But an impasse is reached because each of these reconstructions  
748 is argued for and against based on the same datatypes. There are opportunities for  
749 methodological advances in fields including paleomagnetism, sediment provenance  
750 analysis, and seismology to overcome this impasse, unlocking the 60-25/13 Ma interval  
751 of Tibetan and Himalayan evolution as natural laboratory for typical geological responses  
752 for a-typical post-collisional subduction, or for a-typical geological responses to typical  
753 oceanic subduction.

754

## 755 Acknowledgements

756 I thank my friends and collaborators Wim Spakman, Pete Lippert, Carl Guilmette,  
757 Wentao Huang, Shihu Li, Zhenyu Li, Guillaume Dupont-Nivet, Abdul Qayyum, Paul  
758 Kapp, Thomas Schouten, Licheng Cao, and Eldert Advokaat for the many discussions  
759 that inspired me to write this paper. I thank Alex Webb and two anonymous reviewers for  
760 their critical and constructive suggestions.

761

762 **Funding**

763 This work was supported by Netherlands Organization for Scientific Research Vici grant  
764 865.17.001.

765

766 **Author contributions**

767 DJJvH is the sole author of this paper, performed analyses, and drafted figures.

768

769 **Figure captions**

770

771 **Fig. 1.** Reconstructed India-Asia convergence (20), which, when corrected for Tibetan  
772 shortening (9) predicts Indian plate subduction/underthrusting for the last 60 Ma. The  
773 amount of post-collisional subduction is a function of initial collision age recorded in the  
774 Himalaya (60-55 Ma) (17, 18, 43) and the width of horizontally underthrust India, which  
775 varies along-strike from 400-800 km (at the longitude of the reference location, this width  
776 is ~400 km, Fig. 2).

777

778 **Fig. 2.** Seismic tomographic images taken from the UU-P07 tomography model (48, 99).  
779 **A)** Vertical section from the Indian Ocean to Central Asia (drawn using the Hades  
780 Underworld Explorer, [www.atlas-of-the-underworld.org](http://www.atlas-of-the-underworld.org)). Deep, flat-lying slabs relate to  
781 Mesozoic Paleotethys and Mesotethys subduction during the amalgamation of Tibetan  
782 terranes (14). The India slab contains the bulk of Neotethys lithosphere that subducted  
783 northward below the Lhasa terrane, whereas the northward subducted but overturned  
784 Himalaya slab contains subducted Greater Indian lithosphere (9, 11, 14, 38, 39).  
785 Horizontally underthrust Indian continental lithosphere protrudes northward from the  
786 Main Frontal Thrust over a distance of 400-800 km, varying along-strike (7-10, 14). **B).**  
787 Horizontal cross-section at 110 km depth through the UU-P07 tomography model,  
788 overlain by outlines of modern geology and geography. The yellow dotted line depicts  
789 the outline of the northern margin of horizontally underthrust Indian continent below  
790 Tibet, protruding ~800 km northward north of the Himalayan syntaxes, decreasing to  
791 ~400 km towards ~90°E (7, 9, 10)

792

793 **Fig. 3.** Reconstructions of the diachronous onset of horizontal Indian underthrusting at  
794 **(A)** 28 Ma; **(B)** 15 Ma, and **(C)** the Present Day, using the outline of horizontally  
795 underthrust continental lithosphere of India shown in Figure tomography, using the

796 kinematic reconstruction of Tibet and the Himalaya of reference (9), and India-Asia  
797 convergence following reference (20).

798

799 **Fig. 4.** Paleogeographic maps at the time of initial collision (~60 Ma (17, 18, 43)) and in  
800 Gondwana fits at 155, corresponding to the timing of continental breakup in the Argo  
801 Abyssal Plain between Northwest Australia and the conceptual Argoland continent (50),  
802 for three end-member models discussed in the text. Models are placed in the  
803 paleomagnetic reference frame of reference (100). **A)** Model C, with a fully continental  
804 Greater India (18, 22, 23, 40); **B)** Model A, in which initial collision occurred with an  
805 intra-oceanic subduction zone around the equator. The size of continental Greater India is  
806 here constructed with a 40 Ma closure age of the remaining oceanic lithosphere (6, 24-  
807 27); Model C), in which 60 Ma collision occurs between a microcontinent that broke off  
808 Northern India in the Cretaceous, opening a Greater India Basin in its wake (9, 28). AAP  
809 = Argo Abyssal Plain; CRFZ = Cape Range Fracture Zone; KLA = Kohistan-Ladakh  
810 Arc; PAO = Pakistan Ophiolites; TH = Tibetan Himalaya; WBB = West Burma Block;  
811 WFZ = Wallaby Fracture Zone; XFB = Xigaze Forearc Basin.

812

813 **Fig. 5.** Tectonic map of the India-Asia collision zone, modified after reference (9). Mct =  
814 Main Central Thrust; mft = Main Frontal Thrust; RRF = Red River Fault; std = South  
815 Tibetan Detachment.

816

817 **Fig. 6. A)** Tectonic map of the Himalaya and Tibet, simplified after references (55, 85,  
818 86). **B)** Schematic cross section through the Himalayas and southern Tibet, modified  
819 from reference (6). ATF = Altyn Tagh Fault; GCT = Great Counter Thrust; GT =  
820 Gangdese Thrust; IYSZ = Indus-Yarlung Suture Zone; KF = Karakoram Fault; MCT =  
821 Main Central Thrust; MFT = Main Frontal Thrust; MHT = Main Himalayan Thrust; STD  
822 = South Tibetan Detachment.

823

824 **Fig. 7.** Conceptual evolution of Himalayan architecture if **A)** all Eocene-early Miocene  
825 India-Asia convergence is accommodated to the north of the Himalaya. In this case, the  
826 MCT can have formed when the GH rocks decoupled from their original Indian lower  
827 crustal and lithospheric underpinnings, or **B)**, all or part of the Eocene-early Miocene  
828 India-Asia convergence is accommodated within the Himalaya. In this case, the MCT is  
829 an out-of-sequence thrust that formed within the early Miocene Himalayan fold-thrust  
830 belt and Eocene-Miocene units that may have accreted below the Greater Himalaya have  
831 been removed by subduction erosion.

832

833 **Fig. 8.** Cartoon illustrating geometrical relationships between diachronous slab  
834 detachment and onset of horizontal Indian continental lithospheric underthrusting below  
835 Tibet between 25 and 13 Ma, and geological expressions in the Tibetan Plateau.

836

837 **References**

- 838 1. Cloos, M. Lithospheric buoyancy and collisional orogenesis: Subduction of  
839 oceanic plateaus, continental margins, island arcs, spreading ridges, and seamounts.  
840 *Geological Society of America Bulletin*. 1993; **105**(6): 715-37.
- 841 2. Molnar, P, England, P, Martinod, J. Mantle dynamics, uplift of the Tibetan  
842 Plateau, and the Indian monsoon. *Reviews of Geophysics*. 1993; **31**(4): 357-96.
- 843 3. Xia, L, Li, X, Ma, Z, *et al.* Cenozoic volcanism and tectonic evolution of the  
844 Tibetan plateau. *Gondwana Research*. 2011; **19**(4): 850-66.
- 845 4. Sun, X, Lu, Y, Li, Q, *et al.* A downgoing Indian lithosphere control on along-  
846 strike variability of porphyry mineralization in the Gangdese belt of southern Tibet.  
847 *Economic Geology*. 2021; **116**(1): 29-46.
- 848 5. Nomade, S, Renne, PR, Mo, X, *et al.* Miocene volcanism in the Lhasa block,  
849 Tibet: spatial trends and geodynamic implications. *Earth and Planetary Science Letters*.  
850 2004; **221**(1-4): 227-43.
- 851 6. Kapp, P, DeCelles, PG. Mesozoic–Cenozoic geological evolution of the  
852 Himalayan-Tibetan orogen and working tectonic hypotheses. *American Journal of*  
853 *Science*. 2019; **319**(3): 159-254.
- 854 7. Li, J, Song, X. Tearing of Indian mantle lithosphere from high-resolution seismic  
855 images and its implications for lithosphere coupling in southern Tibet. *Proceedings of the*  
856 *National Academy of Sciences*. 2018; **115**(33): 8296-300.
- 857 8. Chen, M, Niu, F, Tromp, J, *et al.* Lithospheric foundering and underthrusting  
858 imaged beneath Tibet. *Nature communications*. 2017; **8**(1): 1-10.
- 859 9. van Hinsbergen, DJJ, Lippert, PC, Li, S, *et al.* Reconstructing Greater India:  
860 Paleogeographic, kinematic, and geodynamic perspectives. *Tectonophysics*. 2019; **760**:  
861 69-94.
- 862 10. Agius, MR, Lebedev, S. Tibetan and Indian lithospheres in the upper mantle  
863 beneath Tibet: Evidence from broadband surface-wave dispersion. *Geochemistry,*  
864 *Geophysics, Geosystems*. 2013; **14**(10): 4260-81.
- 865 11. Replumaz, A, Negredo, AM, Villaseñor, A, *et al.* Indian continental subduction  
866 and slab break-off during Tertiary collision. *Terra Nova*. 2010; **22**: 290-6.
- 867 12. Nabelek, J, Hetenyi, G, Vergne, J, *et al.* Underplating in the Himalaya-Tibet  
868 collision zone revealed by the Hi-CLIMB experiment. *Science*. 2009; **325**(5946): 1371-4.
- 869 13. Styron, R, Taylor, M, Sundell, K. Accelerated extension of Tibet linked to the  
870 northward underthrusting of Indian crust. *Nature Geoscience*. 2015; **8**(2): 131-4.
- 871 14. Qayyum, A, Lom, N, Advokaat, EL, *et al.* Subduction and slab detachment under  
872 moving trenches during ongoing India- Asia convergence. *Earth and Space Science Open*  
873 *Archive*. 2022: 45.
- 874 15. Webb, AAG, Guo, H, Clift, PD, *et al.* The Himalaya in 3D: Slab dynamics  
875 controlled mountain building and monsoon intensification. *Lithosphere*. 2017.
- 876 16. Ding, L, Kapp, P, Wan, X. Paleocene-Eocene record of ophiolite obduction and  
877 initial India-Asia collision, south central Tibet. *Tectonics*. 2005; **24**(3): n/a-n/a.
- 878 17. An, W, Hu, X, Garzanti, E, *et al.* New precise dating of the India-Asia collision in  
879 the Tibetan Himalaya at 61 Ma. *Geophysical Research Letters*. 2021; **48**(3):  
880 e2020GL090641.

- 881 18. Hu, X, Garzanti, E, Wang, J, *et al.* The timing of India-Asia collision onset –  
882 Facts, theories, controversies. *Earth-Science Reviews*. 2016; **160**: 264-99.
- 883 19. van Hinsbergen, DJJ, Steinberger, B, Doubrovine, PV, *et al.* Acceleration and  
884 deceleration of India-Asia convergence since the Cretaceous: Roles of mantle plumes and  
885 continental collision. *Journal of Geophysical Research*. 2011; **116**(B6).
- 886 20. DeMets, C, Merkuriev, S. Detailed reconstructions of India–Somalia Plate  
887 motion, 60 Ma to present: implications for Somalia Plate absolute motion and India–  
888 Eurasia Plate motion. *Geophysical Journal International*. 2021; **227**(3): 1730-67.
- 889 21. van Hunen, J, Allen, MB. Continental collision and slab break-off: A comparison  
890 of 3-D numerical models with observations. *Earth and Planetary Science Letters*. 2011;  
891 **302**(1-2): 27-37.
- 892 22. Searle, MP. Timing of subduction initiation, arc formation, ophiolite obduction  
893 and India–Asia collision in the Himalaya. *Geological Society, London, Special*  
894 *Publications*. 2018; **483**: SP483. 8.
- 895 23. Ingalls, M, Rowley, DB, Currie, B, *et al.* Large-scale subduction of continental  
896 crust implied by India–Asia mass-balance calculation. *Nature Geoscience*. 2016; **9**(11):  
897 848-53.
- 898 24. Tapponnier, P, Mattauer, M, Proust, F, *et al.* Mesozoic ophiolites, sutures, and  
899 large-scale tectonic movements in Afghanistan. *Earth and Planetary Science Letters*.  
900 1981; **52**(2): 355-71.
- 901 25. Aitchison, JC, Ali, JR, Davis, AM. When and where did India and Asia collide?  
902 *Journal of Geophysical Research*. 2007; **112**(B5).
- 903 26. Martin, CR, Jagoutz, O, Upadhyay, R, *et al.* Paleocene latitude of the Kohistan–  
904 Ladakh arc indicates multistage India–Eurasia collision. *Proceedings of the National*  
905 *Academy of Sciences*. 2020; **117**(47): 29487-94.
- 906 27. Jagoutz, O, Royden, L, Holt, AF, *et al.* Anomalously fast convergence of India  
907 and Eurasia caused by double subduction. *Nature Geoscience*. 2015; **8**(6): 475-8.
- 908 28. van Hinsbergen, DJJ, Lippert, PC, Dupont-Nivet, G, *et al.* Greater India Basin  
909 hypothesis and a two-stage Cenozoic collision between India and Asia. *Proc Natl Acad*  
910 *Sci U S A*. 2012; **109**(20): 7659-64.
- 911 29. Capitanio, FA, Morra, G, Goes, S, *et al.* India–Asia convergence driven by the  
912 subduction of the Greater Indian continent. *Nature Geoscience*. 2010; **3**(2): 136-9.
- 913 30. van Hinsbergen, DJJ, Schouten, TLA. Deciphering paleogeography from orogenic  
914 architecture: constructing orogens in a future supercontinent as thought experiment.  
915 *American Journal of Science*. 2021; **321**: 955-1031.
- 916 31. Cawood, PA, Kröner, A, Collins, WJ, *et al.* Accretionary orogens through Earth  
917 history. *Geological Society, London, Special Publications*. 2009; **318**(1): 1-36.
- 918 32. Borneman, NL, Hodges, KV, Van Soest, MC, *et al.* Age and structure of the  
919 Shyok suture in the Ladakh region of northwestern India: implications for slip on the  
920 Karakoram fault system. *Tectonics*. 2015; **34**(10): 2011-33.
- 921 33. Colleps, C, McKenzie, N, Horton, B, *et al.* Sediment provenance of pre-and post-  
922 collisional Cretaceous–Paleogene strata from the frontal Himalaya of northwest India.  
923 *Earth and Planetary Science Letters*. 2020; **534**: 116079.
- 924 34. Rowley, DB. Comparing Paleomagnetic Study Means with Apparent Wander  
925 Paths: A Case Study and Paleomagnetic Test of the Greater India versus Greater Indian  
926 Basin Hypotheses. *Tectonics*. 2019; **38**: 722-40.



- 927 35. Yuan, J, Yang, Z, Deng, C, *et al.* Rapid drift of the Tethyan Himalaya terrane  
928 before two-stage India-Asia collision. *National Science Review*. 2021; **8**(7): nwaal73.
- 929 36. Jadoon, UF, Huang, B, Shah, SA, *et al.* Multi-stage India-Asia collision:  
930 Paleomagnetic constraints from Hazara-Kashmir syntaxis in the western Himalaya. *GSA*  
931 *Bulletin*. 2021.
- 932 37. Yang, T, Jin, J, Bian, W, *et al.* Precollisional latitude of the Northern Tethyan  
933 Himalaya from the Paleocene redbeds and its implication for greater India and the India-  
934 Asia collision. *Journal of Geophysical Research: Solid Earth*. 2019; **124**(11): 10777-98.
- 935 38. Parsons, AJ, Hosseini, K, Palin, R, *et al.* Geological, geophysical and plate  
936 kinematic constraints for models of the India-Asia collision and the post-Triassic central  
937 Tethys oceans. *Earth-Science Reviews*. 2020: 103084.
- 938 39. Van der Voo, R, Spakman, W, Bijwaard, H. Tethyan subducted slabs under India.  
939 *Earth and Planetary Science Letters*. 1999; **171**(1): 7-20.
- 940 40. Replumaz, A, Tapponnier, P. Reconstruction of the deformed collision zone  
941 Between India and Asia by backward motion of lithospheric blocks. *Journal of*  
942 *Geophysical Research: Solid Earth*. 2003; **108**(B6).
- 943 41. van Hinsbergen, DJJ, Kapp, P, Dupont-Nivet, G, *et al.* Restoration of Cenozoic  
944 deformation in Asia and the size of Greater India. *Tectonics*. 2011; **30**(5): n/a-n/a.
- 945 42. Long, S, McQuarrie, N, Tobgay, T, *et al.* Geometry and crustal shortening of the  
946 Himalayan fold-thrust belt, eastern and central Bhutan. *Geological Society of America*  
947 *Bulletin*. 2011; **123**(7-8): 1427-47.
- 948 43. Guillot, S, Mahéo, G, de Sigoyer, J, *et al.* Tethyan and Indian subduction viewed  
949 from the Himalayan high- to ultrahigh-pressure metamorphic rocks. *Tectonophysics*.  
950 2008; **451**(1-4): 225-41.
- 951 44. McKenzie, D, Priestley, K. The influence of lithospheric thickness variations on  
952 continental evolution. *Lithos*. 2008; **102**(1-2): 1-11.
- 953 45. England, P, Houseman, G. Extension during continental convergence, with  
954 application to the Tibetan Plateau. *Journal of Geophysical Research: Solid Earth*. 1989;  
955 **94**(B12): 17561-79.
- 956 46. Replumaz, A, Guillot, S, Villaseñor, A, *et al.* Amount of Asian lithospheric  
957 mantle subducted during the India/Asia collision. *Gondwana Research*. 2013; **24**(3-4):  
958 936-45.
- 959 47. Feng, J, Yao, H, Chen, L, *et al.* Massive lithospheric delamination in southeastern  
960 Tibet facilitating continental extrusion. *National Science Review*. 2021.
- 961 48. van der Meer, DG, van Hinsbergen, DJJ, Spakman, W. Atlas of the underworld:  
962 Slab remnants in the mantle, their sinking history, and a new outlook on lower mantle  
963 viscosity. *Tectonophysics*. 2018; **723**: 309-448.
- 964 49. Isozaki, Y, Maruyama, S, Furuoka, F. Accreted oceanic materials in Japan.  
965 *Tectonophysics*. 1990; **181**(1-4): 179-205.
- 966 50. Gibbons, AD, Barckhausen, U, van den Bogaard, P, *et al.* Constraining the  
967 Jurassic extent of Greater India: Tectonic evolution of the West Australian margin.  
968 *Geochemistry Geophysics Geosystems*. 2012; **13**.
- 969 51. Agard, P, Yamato, P, Soret, M, *et al.* Plate interface rheological switches during  
970 subduction infancy: Control on slab penetration and metamorphic sole formation. *Earth*  
971 *and Planetary Science Letters*. 2016; **451**: 208-20.

- 972 52. van Hinsbergen, DJJ, Torsvik, T, Schmid, SM, *et al.* Orogenic architecture of the  
973 Mediterranean region and kinematic reconstruction of its tectonic evolution since the  
974 Triassic. *Gondwana Research*. 2020; **81**: 79-229.
- 975 53. Ziabrev, SV, Aitchison, JC, Abrajevitch, AV, *et al.* Bainang Terrane, Yarlung–  
976 Tsangpo suture, southern Tibet (Xizang, China): a record of intra-Neotethyan  
977 subduction–accretion processes preserved on the roof of the world. *Journal of the*  
978 *Geological Society*. 2004; **161**(3): 523-39.
- 979 54. An, W, Hu, X, Garzanti, E. Discovery of Upper Cretaceous Neo-Tethyan trench  
980 deposits in south Tibet (Luogangcuo Formation). *Lithosphere*. 2018; **10**(3): 446-59.
- 981 55. Guilmette, C, Hébert, R, Wang, C, *et al.* Geochemistry and geochronology of the  
982 metamorphic sole underlying the Xigaze Ophiolite, Yarlung Zangbo Suture Zone, South  
983 Tibet. *Lithos*. 2009; **112**(1-2): 149-62.
- 984 56. Garzanti, E. Stratigraphy and sedimentary history of the Nepal Tethys Himalaya  
985 passive margin. *Journal of Asian Earth Sciences*. 1999; **17**(5-6): 805-27.
- 986 57. DeCelles, PG, Kapp, P, Gehrels, GE, *et al.* Paleocene-Eocene foreland basin  
987 evolution in the Himalaya of southern Tibet and Nepal: Implications for the age of initial  
988 India-Asia collision. *Tectonics*. 2014; **33**(5): 824-49.
- 989 58. Donaldson, DG, Webb, AAG, Menold, CA, *et al.* Petrochronology of Himalayan  
990 ultrahigh-pressure eclogite. *Geology*. 2013; **41**(8): 835-8.
- 991 59. Carosi, R, Montomoli, C, Iaccarino, S. 20 years of geological mapping of the  
992 metamorphic core across Central and Eastern Himalayas. *Earth-Science Reviews*. 2018;  
993 **177**: 124-38.
- 994 60. Hodges, KV. Tectonics of the Himalaya and southern Tibet from two  
995 perspectives. *Geological Society of America Bulletin*. 2000; **112**(3): 324-50.
- 996 61. Yin, A. Cenozoic tectonic evolution of the Himalayan orogen as constrained by  
997 along-strike variation of structural geometry, exhumation history, and foreland  
998 sedimentation. *Earth-Science Reviews*. 2006; **76**(1-2): 1-131.
- 999 62. Smit, MA, Hacker, BR, Lee, J. Tibetan garnet records early Eocene initiation of  
1000 thickening in the Himalaya. *Geology*. 2014; **42**(7): 591-4.
- 1001 63. Larson, KP, Ambrose, TK, Webb, AAG, *et al.* Reconciling Himalayan midcrustal  
1002 discontinuities: the Main Central thrust system. *Earth and Planetary Science Letters*.  
1003 2015; **429**: 139-46.
- 1004 64. Grujic, D, Casey, M, Davidson, C, *et al.* Ductile extrusion of the Higher  
1005 Himalayan Crystalline in Bhutan: evidence from quartz microfabrics. *Tectonophysics*.  
1006 1996; **260**(1-3): 21-43.
- 1007 65. Khan, I, Clyde, W. Lower Paleogene Tectonostratigraphy of Balochistan:  
1008 Evidence for Time-Transgressive Late Paleocene-Early Eocene Uplift. *Geosciences*.  
1009 2013; **3**(4): 466-501.
- 1010 66. Qasim, M, Ahmad, J, Ding, L, *et al.* Integrated provenance and tectonic  
1011 implications of the Cretaceous–Palaeocene clastic sequence, Changla Gali, Lesser  
1012 Himalaya, Pakistan. *Geological Journal*. 2021; **56**(9): 4747-59.
- 1013 67. Gaina, C, van Hinsbergen, DJJ, Spakman, W. Tectonic interactions between India  
1014 and Arabia since the Jurassic reconstructed from marine geophysics, ophiolite geology,  
1015 and seismic tomography. *Tectonics*. 2015; **34**(5): 875-906.

- 1016 68. Robinson, DM, DeCelles, PG, Copeland, P. Tectonic evolution of the Himalayan  
1017 thrust belt in western Nepal: Implications for channel flow models. *Geological Society of*  
1018 *America Bulletin*. 2006; **118**(7-8): 865-85.
- 1019 69. Beaumont, C, Jamieson, RA, Nguyen, M, *et al.* Himalayan tectonics explained by  
1020 extrusion of a low-viscosity crustal channel coupled to focused surface denudation.  
1021 *Nature*. 2001; **414**(6865): 738-42.
- 1022 70. Xiao, W, Ao, S, Yang, L, *et al.* Anatomy of composition and nature of plate  
1023 convergence: Insights for alternative thoughts for terminal India-Eurasia collision.  
1024 *Science China Earth Sciences*. 2017; **60**(6): 1015-39.
- 1025 71. Jagoutz, O, Bouilhol, P, Schaltegger, U, *et al.* The isotopic evolution of the  
1026 Kohistan Ladakh arc from subduction initiation to continent arc collision. *Geological*  
1027 *Society, London, Special Publications*. 2019; **483**(1): 165-82.
- 1028 72. Orme, DA. Burial and exhumation history of the Xigaze forearc basin, Yarlung  
1029 suture zone, Tibet. *Geoscience Frontiers*. 2019; **10**(3): 895-908.
- 1030 73. Einsele, G, Liu, B, Dürr, S, *et al.* The Xigaze forearc basin: evolution and facies  
1031 architecture (Cretaceous, Tibet). *Sedimentary Geology*. 1994; **90**(1-2): 1-32.
- 1032 74. Huang, W, van Hinsbergen, DJJ, Maffione, M, *et al.* Lower Cretaceous Xigaze  
1033 ophiolites formed in the Gangdese forearc: Evidence from paleomagnetism, sediment  
1034 provenance, and stratigraphy. *Earth and Planetary Science Letters*. 2015; **415**: 142-53.
- 1035 75. Yin, A, Harrison, TM, Ryerson, F, *et al.* Tertiary structural evolution of the  
1036 Gangdese thrust system, southeastern Tibet. *Journal of Geophysical Research: Solid*  
1037 *Earth*. 1994; **99**(B9): 18175-201.
- 1038 76. Maffione, M, van Hinsbergen, DJJ, Koornneef, LMT, *et al.* Forearc  
1039 hyperextension dismembered the south Tibetan ophiolites. *Geology*. 2015; **43**(6): 475-8.
- 1040 77. Li, Y, Li, R, Robinson, P, *et al.* Detachment faulting in the Xigaze ophiolite  
1041 southern Tibet: New constraints on its origin and implications. *Gondwana Research*.  
1042 2021; **94**: 44-55.
- 1043 78. Yin, A, Harrison, TM. Geologic evolution of the Himalayan-Tibetan orogen.  
1044 *Annual Review of Earth and Planetary Sciences*. 2000; **28**(1): 211-80.
- 1045 79. Murphy, MA, Yin, A, Harrison, TM, *et al.* Did the Indo-Asian collision alone  
1046 create the Tibetan plateau? *Geology*. 1997; **25**(8).
- 1047 80. Li, S, van Hinsbergen, DJ, Najman, Y, *et al.* Does pulsed Tibetan deformation  
1048 correlate with Indian plate motion changes? *Earth and Planetary Science Letters*. 2020;  
1049 **536**: 116144.
- 1050 81. Kapp, P, DeCelles, PG, Gehrels, GE, *et al.* Geological records of the Lhasa-  
1051 Qiangtang and Indo-Asian collisions in the Nima area of central Tibet. *Geological*  
1052 *Society of America Bulletin*. 2007; **119**(7-8): 917-33.
- 1053 82. Cowgill, E. Cenozoic right-slip faulting along the eastern margin of the Pamir  
1054 salient, northwestern China. *Geological Society of America Bulletin*. 2010; **122**(1-2):  
1055 145-61.
- 1056 83. Bullen, M, Burbank, D, Garver, J. Building the northern Tien Shan: Integrated  
1057 thermal, structural, and topographic constraints. *The Journal of Geology*. 2003; **111**(2):  
1058 149-65.
- 1059 84. Xiao, G, Guo, Z, Dupont-Nivet, G, *et al.* Evidence for northeastern Tibetan  
1060 Plateau uplift between 25 and 20 Ma in the sedimentary archive of the Xining Basin,  
1061 Northwestern China. *Earth and Planetary Science Letters*. 2012; **317**: 185-95.

- 1062 85. DeCelles, PG, Kapp, P, Quade, J, *et al.* Oligocene-Miocene Kailas basin,  
1063 southwestern Tibet: Record of postcollisional upper-plate extension in the Indus-Yarlung  
1064 suture zone. *Geological Society of America Bulletin*. 2011; **123**(7-8): 1337-62.
- 1065 86. Leary, R, Orme, DA, Laskowski, AK, *et al.* Along-strike diachroneity in  
1066 deposition of the Kailas Formation in central southern Tibet: Implications for Indian slab  
1067 dynamics. *Geosphere*. 2016; **12**(4): 1198-223.
- 1068 87. Li, S, Advokaat, EL, van Hinsbergen, DJJ, *et al.* Paleomagnetic constraints on the  
1069 Mesozoic-Cenozoic paleolatitudinal and rotational history of Indochina and South China:  
1070 Review and updated kinematic reconstruction. *Earth-Science Reviews*. 2017; **171**: 58-77.
- 1071 88. Bagheri, S, Gol, SD. The Eastern Iranian Orocline. *Earth-Science Reviews*. 2020:  
1072 103322.
- 1073 89. Coleman, M, Hodges, K. Evidence for Tibetan plateau uplift before 14 Myr ago  
1074 from a new minimum age for east–west extension. *Nature*. 1995; **374**(6517): 49-52.
- 1075 90. Gan, W, Molnar, P, Zhang, P, *et al.* Initiation of clockwise rotation and eastward  
1076 transport of southeastern Tibet inferred from deflected fault traces and GPS observations.  
1077 *GSA Bulletin*. 2021.
- 1078 91. Taylor, M, Yin, A. Active structures of the Himalayan-Tibetan orogen and their  
1079 relationships to earthquake distribution, contemporary strain field, and Cenozoic  
1080 volcanism. *Geosphere*. 2009; **5**(3): 199-214.
- 1081 92. Clark, MK, Royden, LH. Topographic ooze: Building the eastern margin of Tibet  
1082 by lower crustal flow. *Geology*. 2000; **28**(8).
- 1083 93. van Hinsbergen, DJJ, Spakman, W, de Boorder, H, *et al.* Arc-type magmatism  
1084 due to continental-edge plowing through ancient subduction-enriched mantle.  
1085 *Geophysical Research Letters*. 2020; **47**(9): e2020GL087484.
- 1086 94. Shen, T, Wang, G, Replumaz, A, *et al.* Miocene subsidence and surface uplift of  
1087 southernmost Tibet induced by Indian subduction dynamics. *Geochemistry, Geophysics,*  
1088 *Geosystems*. 2020; **21**(10): e2020GC009078.
- 1089 95. Vaes, B, Gallo, LC, van Hinsbergen, DJJ. On pole position: causes of dispersion  
1090 of the paleomagnetic poles behind apparent polar wander paths. *Journal of Geophysical*  
1091 *Research*. 2022.
- 1092 96. Saylor, JE, Sundell, KE. Quantifying comparison of large detrital geochronology  
1093 data sets. *Geosphere*. 2016; **12**(1): 203-20.
- 1094 97. Cai, F, Ding, L, Laskowski, AK, *et al.* Late Triassic paleogeographic  
1095 reconstruction along the Neo–Tethyan Ocean margins, southern Tibet. *Earth and*  
1096 *Planetary Science Letters*. 2016; **435**: 105-14.
- 1097 98. Wei, SS, Shearer, PM, Lithgow-Bertelloni, C, *et al.* Oceanic plateau of the  
1098 Hawaiian mantle plume head subducted to the uppermost lower mantle. *Science*. 2020;  
1099 **370**(6519): 983-7.
- 1100 99. Amaru, M. *Global travel time tomography with 3-D reference models*: Utrecht  
1101 University; 2007.
- 1102 100. Torsvik, TH, Van der Voo, R, Preeden, U, *et al.* Phanerozoic polar wander,  
1103 palaeogeography and dynamics. *Earth-Science Reviews*. 2012; **114**(3-4): 325-68.

1104

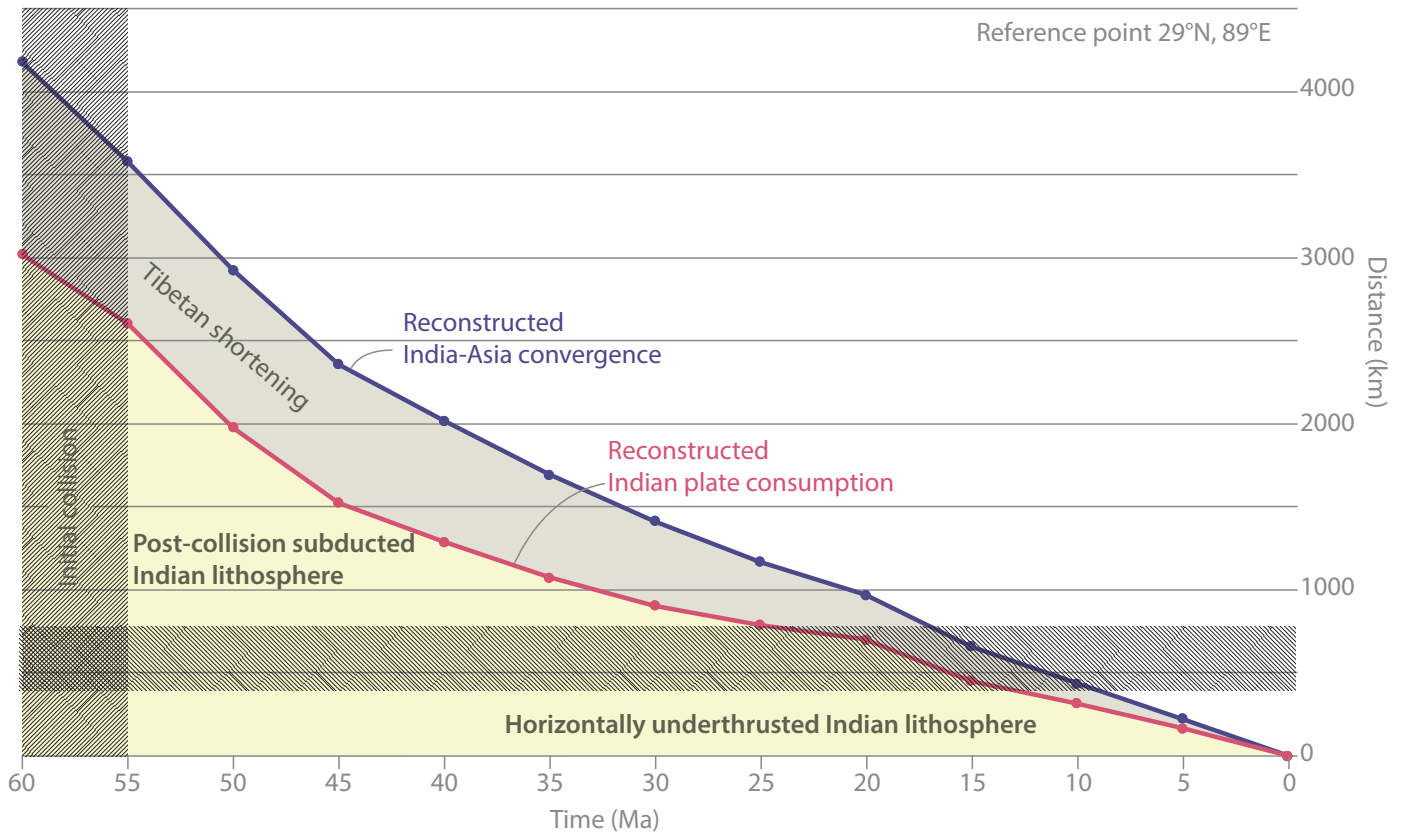


Figure 1

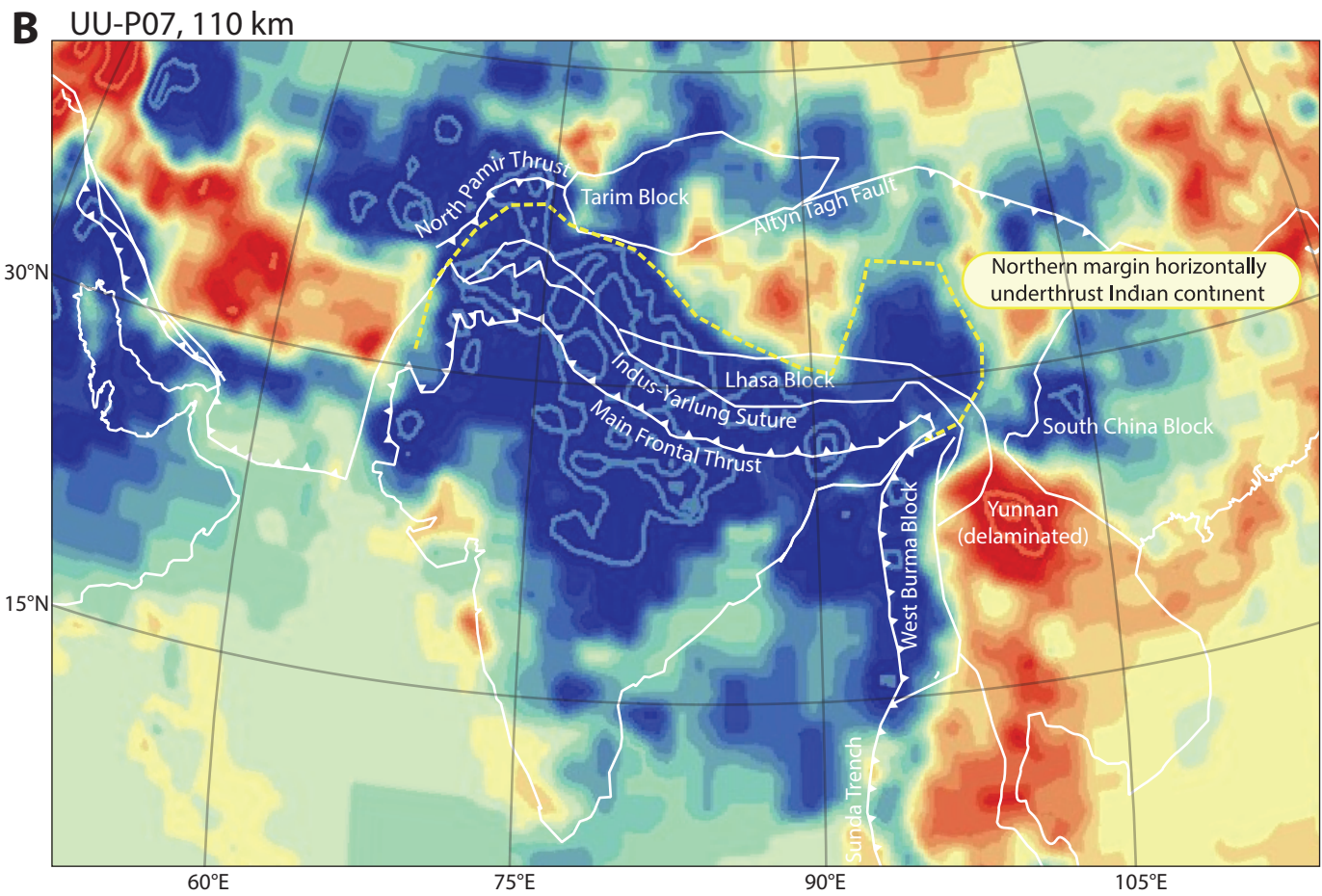
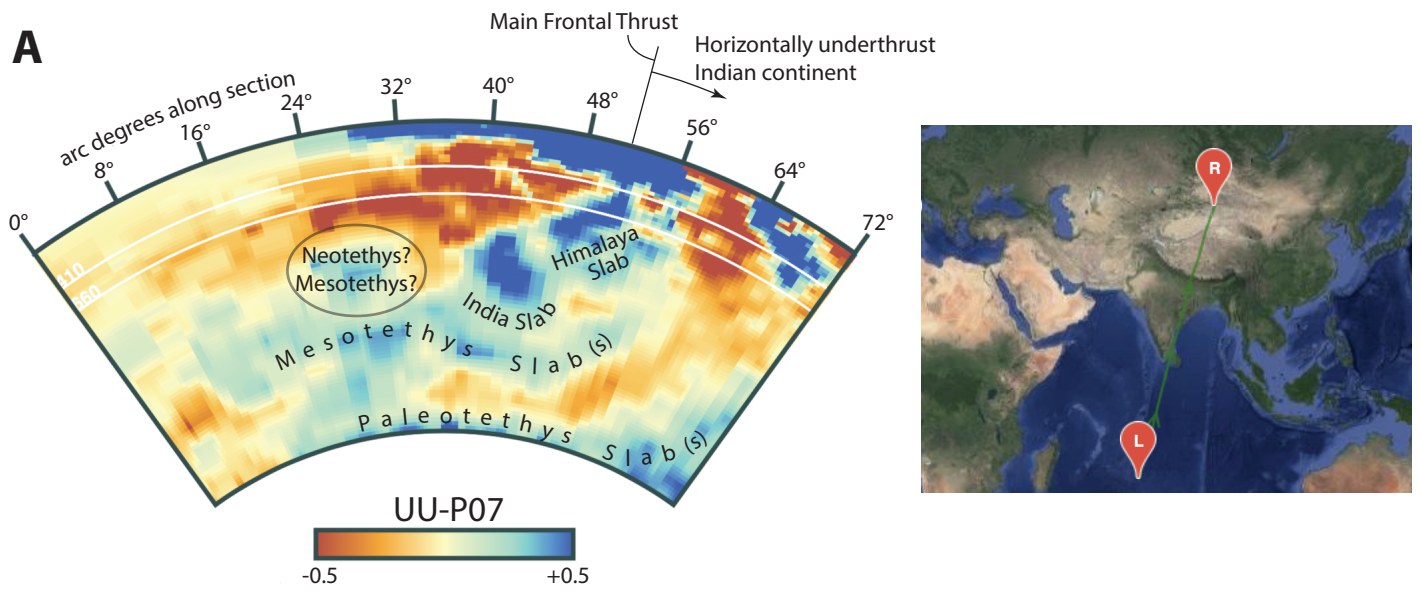


Figure 2

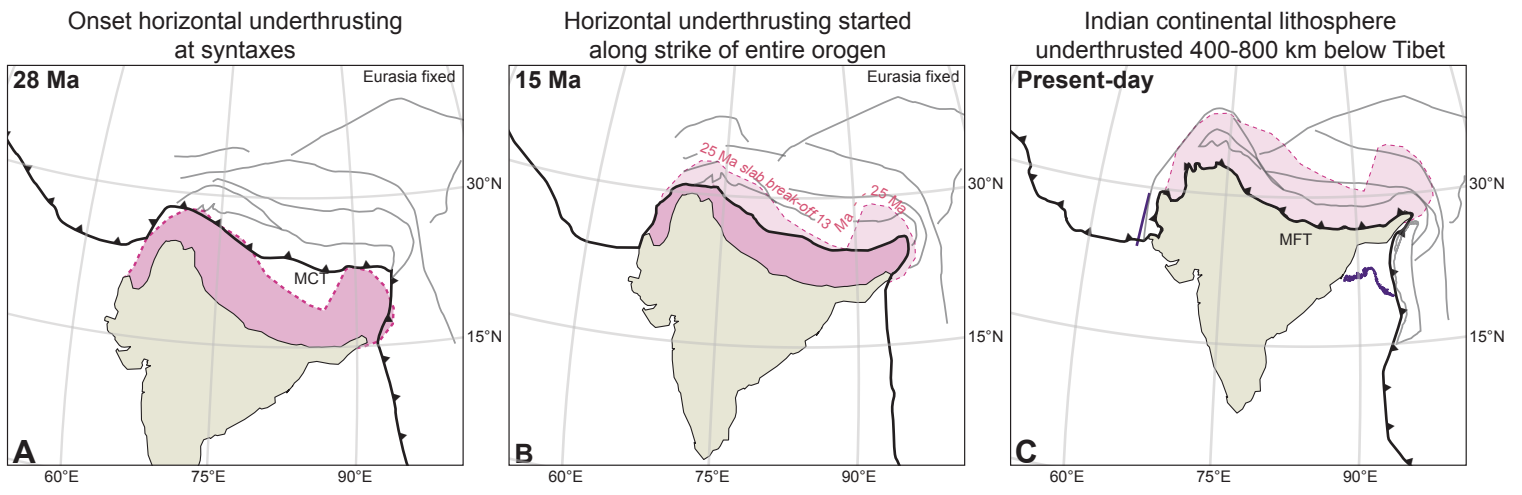


Figure 3

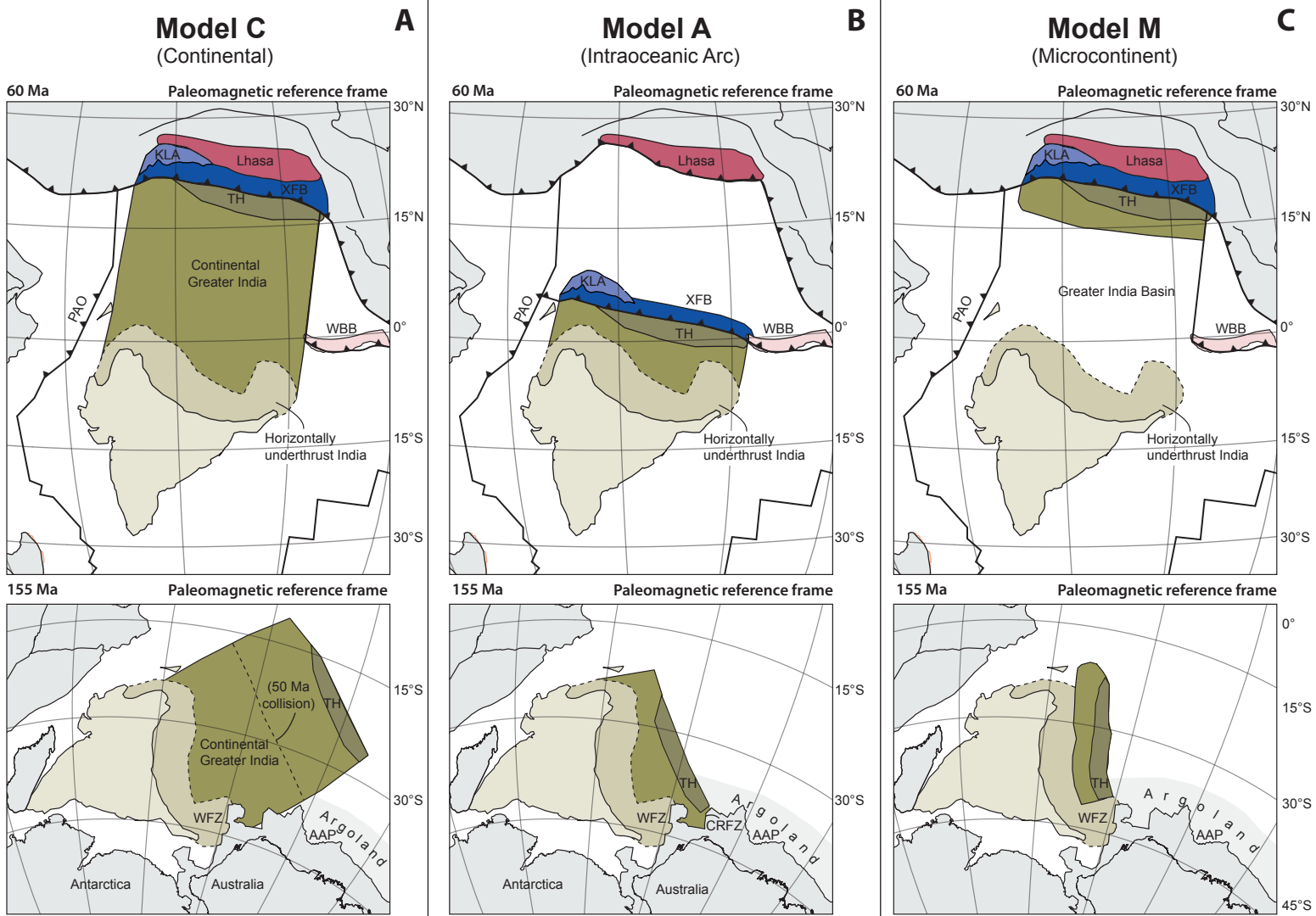


Figure 4



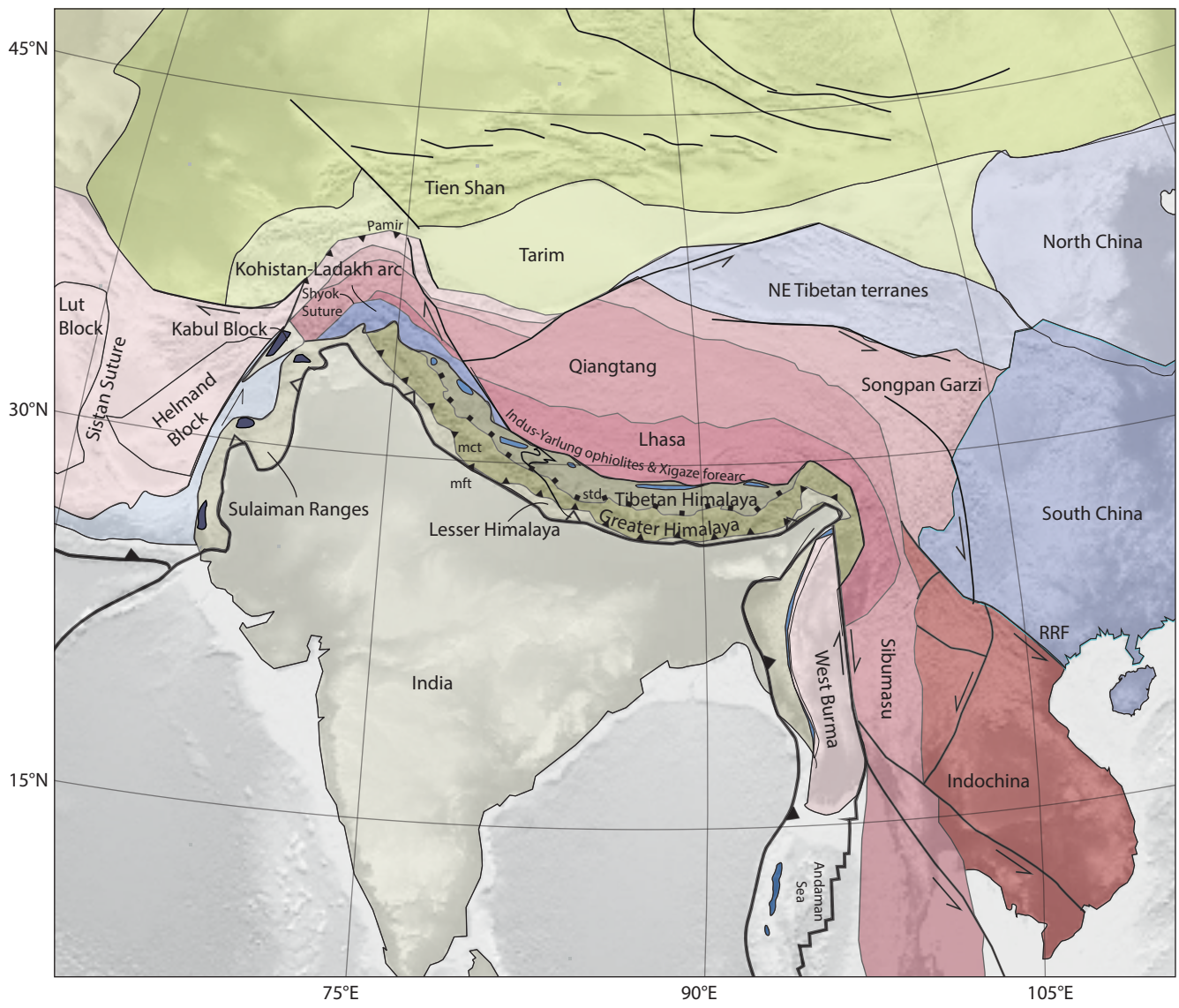


Figure 5

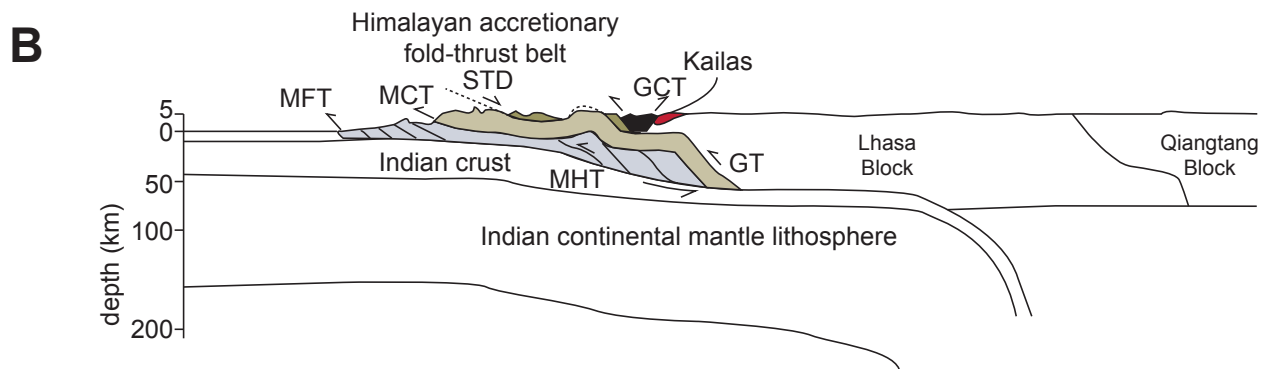
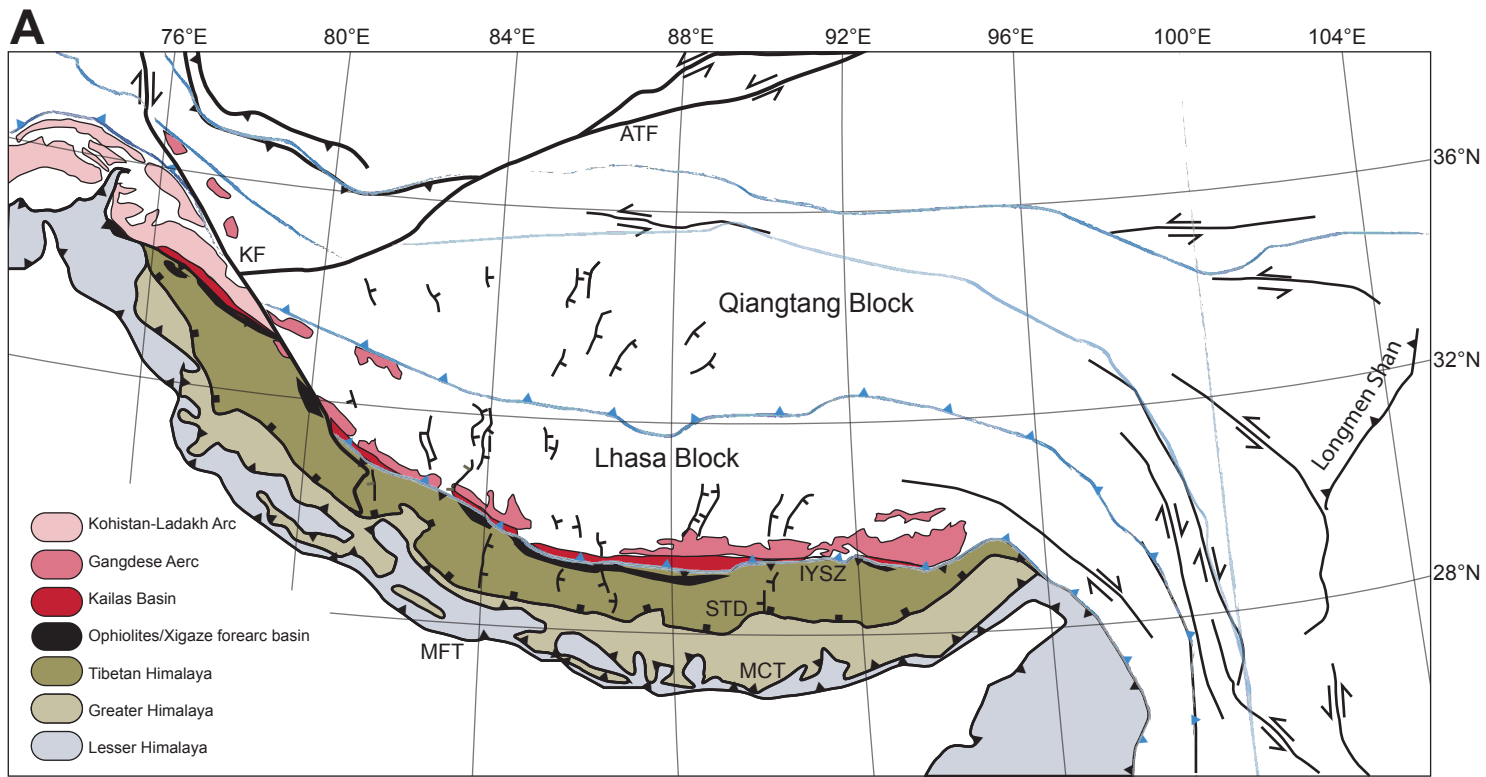
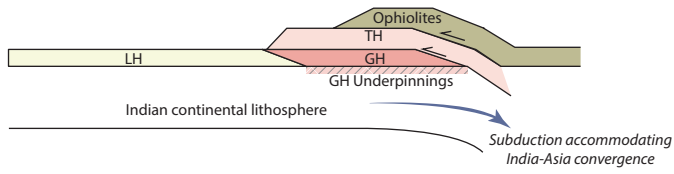


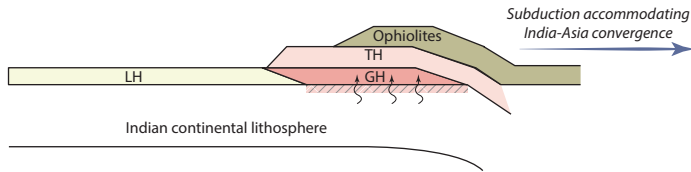
Figure 6

**A. Eocene-Miocene India-Asia convergence accommodated to the north of the Himalaya**

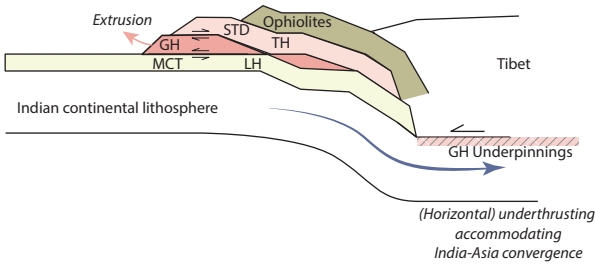
Late Paleocene-Early Eocene



Early Eocene-Early Miocene

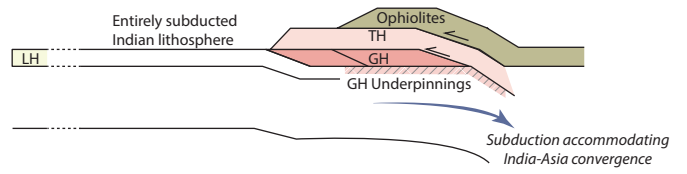


Early-Middle Miocene

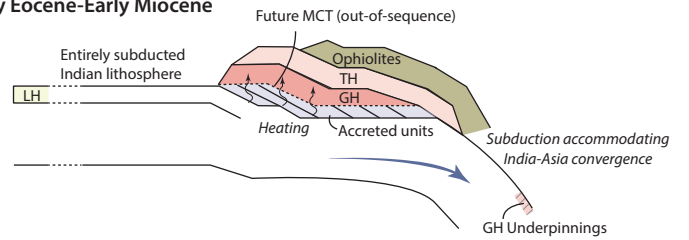


**B. Eocene-Miocene India-Asia convergence (partly) accommodated within the Himalaya**

Late Paleocene-Early Eocene



Early Eocene-Early Miocene



Early-Middle Miocene

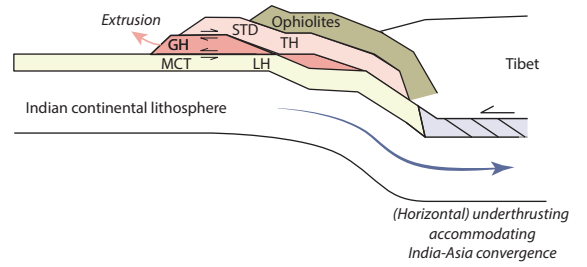


Figure 7

# Miocene diachronous slab detachment and onset of horizontal underthrusting below Tibet

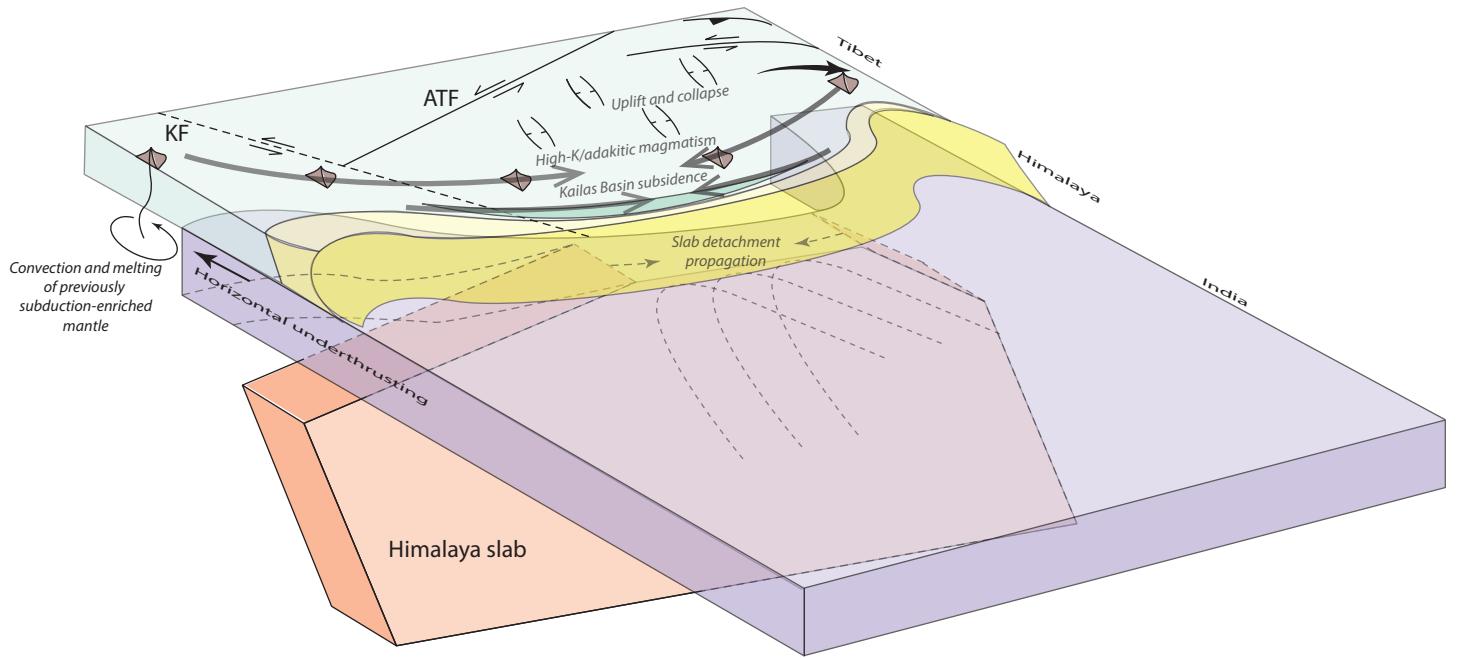


Figure 8